Nano Today xxx (2016) xxx–xxx

Contents lists available at ScienceDirect

Nano Today

journal homepage: www.elsevier.com/locate/nanotoday

Review

# Tribotronics—A new field by coupling triboelectricity and semiconductor

Chi Zhang [a,**], Zhong Lin Wang [a,b,*]

[a] Beijing Institute of Nanoenergy and Nanosystems, Chinese Academy of Sciences; National Center for Nanoscience and Technology, Beijing 100083, PR China
[b] School of Material Science and Engineering, Georgia Institute of Technology, Atlanta, GA 30332-0245, USA

ARTICLE INFO

*Article history:*
Received 26 April 2016
Received in revised form 1 July 2016
Accepted 9 July 2016
Available online xxx

*Keywords:*
Nanogenerator
Contact electrification
Field effect transistor
Tribotronics
Tribophotonics
Tribo-phototronics

ABSTRACT

Contact electrification between two different materials results in a potential difference when they are separated, which has been used as a driving force for energy conversion as a result of invention of triboelectric nanogenerator (TENG). Here, by coupling the triboelectricity with semiconductor, a new field of tribotronics has been proposed in 2014, which is about the devices fabricated using the electrostatic potential created by triboelectrification as a "gate" voltage to tune/control electrical transport and transformation in semiconductors. Various tribotronic functional devices have been developed, such as tribotronic logic circuits, memory, LED and phototransistor, with a variety of materials, including silicon, flexible organic, $MoS_2$, etc. As an extension of the proposed piezoelectric nanogenerator in 2006, piezotronics in 2007 and triboelectric nanogenerator in 2012, tribotronics is another original and novel field in the development of nano-energy and nano-electronics. The concepts and results presented in this review show promises for implementing novel micro/nano-electromechanical devices that may derive plenty of potentially important research interests and applications in sensing, energy harvesting, human-machine interfacing, MEMS/NEMS and active flexible/stretchable electronics in the near future.



**Contents**



* Corresponding authors at: Beijing Institute of Nanoenergy and Nanosystems, Chinese Academy of Sciences; National Center for Nanoscience and Technology, Beijing 100083, PR China.
** Corresponding author.
*E-mail addresses:* czhang@binn.cas.cn (C. Zhang), zlwang@gatech.edu (Z.L. Wang).

http://dx.doi.org/10.1016/j.nantod.2016.07.004
1748-0132/

## Introduction

### *Nanogenerators and piezotronics*

In recent years, sensor network and personalized service have been predicted as the major driving force for industry. Electronics is developing towards personal, portable and flexible, and has great demands for diversity and multifunctionality in the future [1]. The conventional electronics such as field effect transistors (FETs) need to be modulated by the electrical signal, but cannot be directly triggered by human/ambient environment [2,3]. With the integration of multifunctional sensing system and self-powering technology, it is expecting in near future to generate electrical signal from external mechanical energy and realize direct interaction between human/ambient and electronics.

Over the past decade, Prof. Zhong Lin Wang's research group has been devoting to the fields of nano-energy and nano-electronics, and demonstrated several groundbreaking inventions and discoveries by utilizing nanomaterials and nanotechnology to convert ambient mechanical energy into electricity for self-powered systems and active sensors [1,4,5]. In 2006, by scanning across vertical piezoelectric ZnO nanowire arrays with a conductive atomic force microscope (AFM) tip, a nanogenerator as the world's smallest generator was first invented for converting nanoscale mechanical energy into electricity (Fig. 1a) [6]. The mechanism of the nanogenerator relies on the piezoelectric potential created in the nanowires by an external strain, which has laid a foundation of nanoelectronics with functional diversity and opened the door to a new field of nano-energy. On the basis of the piezoelectric semiconductor materials such as ZnO, GaN and CdS with wurtzite or zinc blende structure, the emerging field of piezotronics was first proposed in 2007 [7–12]. Piezotronic effect is to use the piezopotential as a "gate" voltage to tune/control charge carrier transport at a contact or junction, which is the coupling of piezoelectric polarization with semiconductor properties (Fig. 1b) [13]. By further introducing photo excitation, piezo-phototronic effect is to use the piezopotential to tune/control the charge generation, separation, transport and/or recombination at an interface/junction for achieving superior optoelectronic processes, which has also been proposed in 2010 [14,15]. By establishing the direct interaction mechanism between the external strain and electronic/photoelectronic devices, the piezotronics and piezo-phototronics have enormous applications in sensing, human-computer interaction, stress imaging and communication [16–25].

Since 2012, the triboelectric nanogenerator (TENG) has been invented for converting ambient mechanical energy into electricity, which is much different from the piezoelectric nanogenerator [26–32]. The working principle of the TENG is based on the coupling of contact electrification and electrostatic induction, which can induce the charge transfer between two dielectric films in contact with opposite tribo-polarity and generate a potential difference when they are separated. The potential difference would drive free electrons flow from one electrode to the other electrode connected by an external load (Fig. 1c). For a single layer TENG of 3 $cm^2$, the output voltage can reach 200–1000 V and the output current is 100 μA, which can light up hundreds of LEDs, drive wireless sensing system and charge mobile phone battery [33,34]. The TENG has great advantages of polymer-based flexible, easy processing, long life, compatible with other technologies, and larger output power than the piezoelectric nanogenerator, which can be used as a sustainable power supply for enormous potential applications, including but not limited to personal electronics, environmental monitoring, health devices, and medical science.

### *Applications of TENG*

Since the TENG was invented in 2012, different modes and structures have been illustrated depending on specific applications. The first and direct goal of TENGs is to power micro and small electronics. By developing various prototypes such as rotary disk [35], radial grating [36], fabrics [37], and multilayered films [38] (Fig. 2a), the TENG can be used as a micro-scale power source by harvesting multiform ambient mechanical energy, including hand pressing, body motion, human walking, machine vibration, and wheel moving [39–43].

The TENG has also been used for harvesting energy from flowing water in river, rain drops, tide and ocean waves, which has demonstrated enormous potential for general power application at large-scale [44–48]. By constructing a network of the TENGs, an average output power of more than 1 MW from 1 $km^2$ surface area can be expected for harvesting wave energy [49,50] (Fig. 2b). This innovative and effective approach possibly prompts the TENG to the mega-scale blue energy harvesting from the ocean in the near future.

Moreover, as the TENG converts a mechanical trigger into an electric signal, it can be used as a self-powered active sensor for sensing a dynamic mechanical action without power supply [51–53]. The TENGs have been applied as various active sensors, such as self-powered wireless sensing node [54], transparent paper-based page mark and anti-theft sensor [55], self-powered velocity and trajectory tracking sensor array [56], and self-powered vehicle collision acceleration sensor [57] (Fig. 2c).

Recently, the TENG has demonstrated the symmetry and complementary with the traditional electromagnetic induction generator (EMIG) in mechanisms and characteristics [58,59], which has great advantages of high output voltage for capacitive devices, such as micro-actuators [60], ultraviolet emitter [61], and particulate matter filter [62]. The TENG can be a role in place of the conventional voltage supply for capacitive devices, which could be very useful and interesting in conjunction with electronics.

Here in this review, we focus on the recent developments of tribotronics, which is a new field by coupling triboelectricity and semiconductor. Following the proposed piezoelectric nanogenerator in 2006, piezotronics in 2007 and triboelectric nanogenerator in 2012, tribotronics was first proposed in 2014, which is also a new application of TENG as a control source. Firstly, the contact electrification field-effect transistor by coupling TENG and traditional field-effect transistor is reviewed, which is the fundamental component of tribotronics. Then we primarily elaborate on the latest progress of tribotronic devices in terms of functionality and material diversification, as well as the applications for active interactions between human/ambient and electronics. Moreover, we summarized the theoretical analysis of some tribotronic functional devices and their performances. Perspectives and opportunities for future

Please cite this article in press as: C. Zhang, Z.L. Wang, Tribotronics—A new field by coupling triboelectricity and semiconductor, Nano Today (2016), http://dx.doi.org/10.1016/j.nantod.2016.07.004

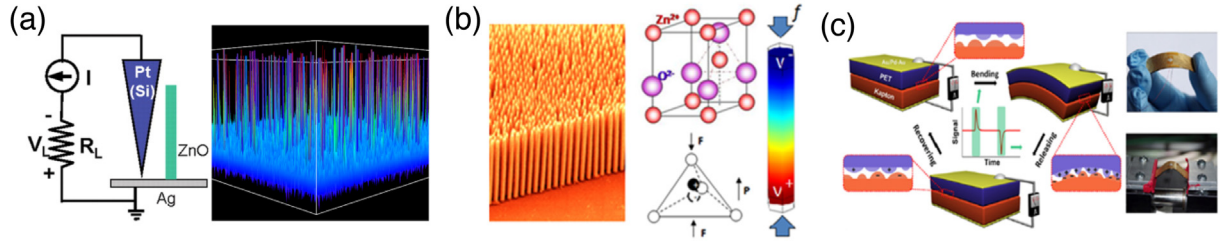


**Fig. 1.** Groundbreaking studies on piezoelectric nanogenerator, piezotronics and triboelectric nanogenerator. (a) Experimental setup and output voltages image by scanning across vertical piezoelectric ZnO nanowire arrays with a conductive AFM tip for first converting nanoscale mechanical energy into electricity. (Reprinted with permission from Ref. [6]. Copyright 2006 The American Association for the Advancement of Science) (b) Wurtzite structure model and piezopotential distribution of a vertical ZnO nanowire with non-central symmetry as the basic physics of piezotronic effect. (Reprinted with permission from Ref. [13]. Copyright 2009 Elsevier Ltd.) (c) Structure and electrical measurement of the first flexible TENG in bending and releasing process. Photographic images of the TENG and experimental setup. (Reprinted with permission from Ref. [26]. Copyright 2012 Elsevier Ltd.).

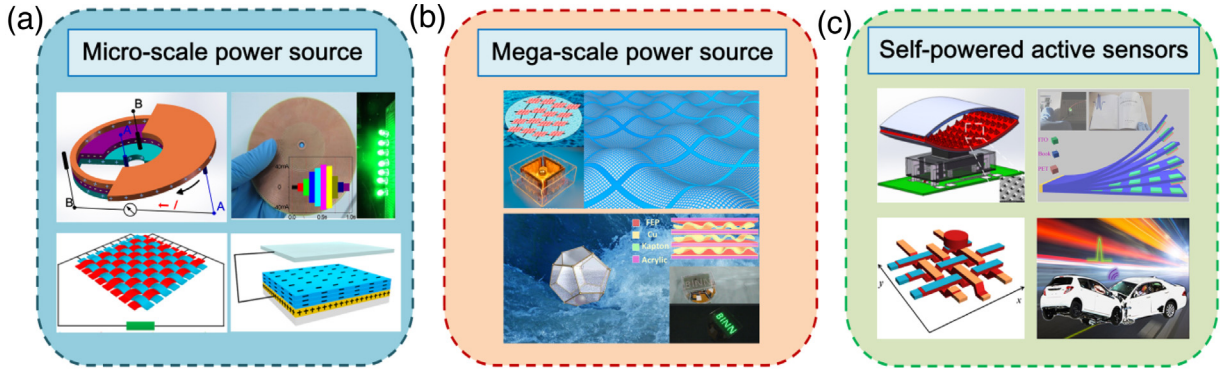


**Fig. 2.** Key fields of applications of TENG. (a) TENGs as micro-scale power source. The insets are rotating-disk-based direct-current TENG, printed circuit board based TENG, woven structured TENG, and multilayered electret films based TENG for powering small electronics. (Reprinted with permission from Ref. [35]. Copyright 2014 John Wiley & Sons, Inc. Reprinted with permission from Ref. [36]. Copyright 2015 Springer. Reprinted with permission from Ref. [37]. Copyright 2014 American Chemical Society. Reprinted with permission from Ref. [38]. Copyright 2016 Springer.) (b) TENGs as mega-scale power source. The insets are cube and dodecahedron structured TENGs and network design for large-scale harvesting of kinetic water energy. (Reprinted with permission from Ref. [49]. Copyright 2015 American Chemical Society. Reprinted with permission from Ref. [50]. Copyright 2016 Elsevier Ltd.) (c) TENGs as self-powered sensors. The insets are self-powered wireless sensing node, transparent paper-based page mark and anti-theft sensor, self-powered velocity and trajectory tracking sensor array, and self-powered vehicle collision acceleration sensor. (Reprinted with permission from Ref. [54]. Copyright 2014 IOP Publishing Ltd. Reprinted with permission from Ref. [55]. Copyright 2014 Springer. Reprinted with permission from Ref. [56]. Copyright 2014 Elsevier Ltd. Reprinted with permission from Ref. [57]. Copyright 2015 American Chemical Society.). Reprinted with permission from Ref. [67]. Copyright 2014 American Chemical Society.

development and applications of tribotronics are also discussed in conclusion.

## Contact electrification field effect transistor—a fundamental component of tribotronics

Piezoelectric and electrostatic micro-actuators are both capacitive devices in micromechanics. While in the microelectronics, there is a common capacitive structure of metal-insulator-semiconductor (MIS), which is the basic structure in metal-oxide-semiconductor field effect transistor (MOSFET) [63–66]. The conduction channel width or charge carrier concentration in the semiconductor layer is controlled by the externally applied gate voltage, and then the drain-source current can be modulated, which is the basic working principle of the MOSFET. For the conventional MOSFET, if the TENG replaces of the gate voltage source to modulate the MIS capacitor, it is expecting that the drain-source current could be directly controlled by the external mechanical energy.

Based on this idea, the contact electrification field effect transistor (CE-FET) was invented, which is composed of a back-gate silicon-on-insulator (SOI) MOSFET and a mobile layer [67]. Different from the conventional back gate MOSFET, the externally applied gate voltage source is replaced by the mobile layer, which consists of a Kapton film and an aluminum electrode and can vertically contact to and separate from the gate electrode by the external force (Fig. 3a). When the Kapton film contacts with the gate electrode, the aluminum has positive charges while the Kapton has negative charges. When the mobile layer gradually separated, the electron will flow from mobile aluminum to the source electrode for the electrostatic induction, resulting in a positive inner gate voltage for the back-gated MOSFET. The relationship between the inner positive gate voltage $V_G$ and the gap $d$ are described by the following equation [67]:

$$V_G = \frac{\varepsilon_K \times Q_0 \times d}{\varepsilon_0 \times \varepsilon_K \times S_0 + \varepsilon_0 \times C_{MIS} \times d_K + \varepsilon_K \times C_{MIS} \times d} \quad (1)$$

where $Q_0$ is the frictional surface charge quantity, $S_0$ is the frictional surface area, $\varepsilon_0$ and $\varepsilon_K$ are the dielectric constant of vacuum and Kapton, $d_K$ is the thickness of the Kapton film, and $C_{MIS}$ is the MIS capacitance. Therefore, a depletion zone will be formed, which will decrease the channel width and thus the drain current (Fig. 3b). The CE-FET can be considered as the coupling of the MOSFET and TENG (Fig. 3c), in which the inner gate voltage can be generated and the carrier transport between drain and source can be tuned/controlled by the external contact instead of the conventional gate voltage (Fig. 3d). With the mobile layer is vertically separated by 80 μm, the drain current is decreased from 13.4 to 1.9 μA at a drain voltage of 5 V in this depletion mode (Fig. 3e). Alternatively, if the Kapton film is attached to the back side of the gate electrode and the mobile layer is only a piece of aluminum film, a negative inner gate voltage can be generated and the carrier concentration in the conduction channel will be increased. With the mobile layer is vertically sepa-

Please cite this article in press as: C. Zhang, Z.L. Wang, Tribotronics—A new field by coupling triboelectricity and semiconductor, Nano Today (2016), http://dx.doi.org/10.1016/j.nantod.2016.07.004

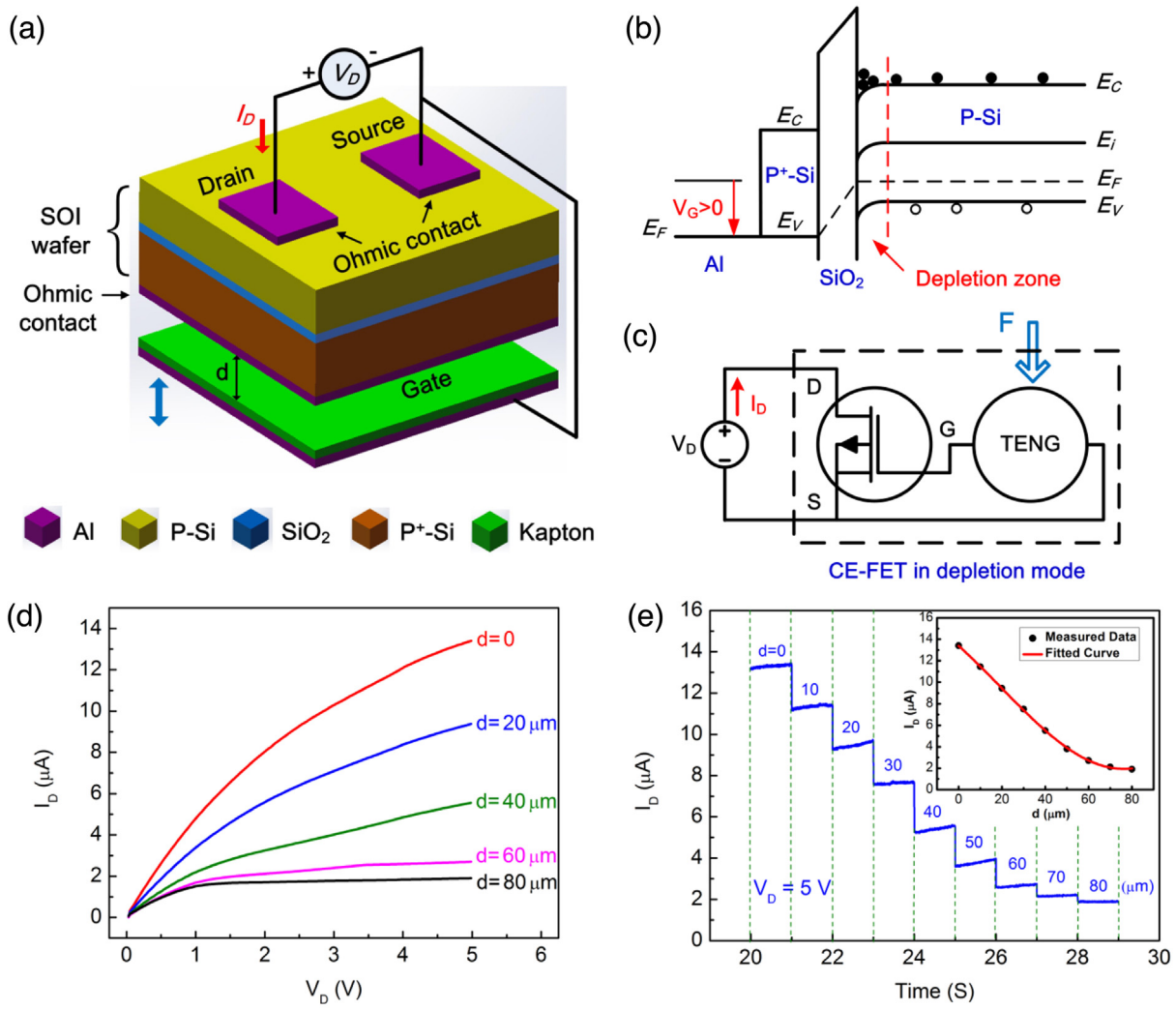


**Fig. 3.** Contact electrification field-effect transistor (CE-FET). (a) Schematic diagram of the CE-FET. (b) Equivalent circuit of the CE-FET. (c) Energy diagram of the MIS capacitor in the CE-FET at the gate voltage. (d) $I_D$-$V_D$ output characteristics at different vertical distances. (e) $I_D$-$t$ output characteristics with the change of the vertical distance. The inset is $I_D$-$d$ transfer characteristic.

rated by 80 μm, the drain current is increased from 2.4 to 12.1 μA at a drain voltage of 5 V in this enhancement mode.

The CE-FET has established a direct interaction mechanism between the external environment and electronics, and provided a new approach for sensors, human-silicon technology interfacing, micro/nano-electro-mechanical systems (MEMS/NEMS), nanorobotics, and active flexible electronics. The CE-FET is compared to the traditional FET and piezotronic transistor (Table 1). The CE-FET and piezotronic transistor are both the two-terminal semiconductor devices, in which the external mechanical force has replaced the traditional third terminal of FET and directly created an inner electric field to tune/control the current carrier transport characteristics. The difference is that the self-generated inner piezopotential controls the interface/junction of the piezotronic transistor, while the self-generated inner triboelectric potential controls the channel width of the CE-FET as in the conventional FET. Because the TENG can provide higher output voltage than the piezoelectric nanogenerator, and the selected materials of the CE-FET can be expanded to general semiconductors and any materials for contact electrification, the CE-FET has been considered to have a larger sensing range for the external environment, far more choice of materials, and wider application prospects in conjunction with the conventional semiconductor devices than the piezotronic transistor.

As a fundamental component, the CE-FET could derive a series of interactive functional devices and open up a new field of tribotronics. Tribotronics is about the devices fabricated using the electrostatic potential created by triboelectrification as a "gate" voltage to tune/control electrical transport and transformation in semiconductors for human-machine interaction. Tribotronics is a field by coupling the triboelectricity with semiconductor, and also a new application of TENG as the triboelectric-voltage-controlled electronics. As another original and novel invention, together with piezotronics, tribotronics will lay important foundations for the development of intelligent interfacing in the human-machine interaction technology.

## Tribotronic functional devices

### *Tribotronic logic circuits and basic operations*

Based on the CE-FET, the tribotronic logic circuits have been developed for demonstrating the combinational logic operations [68]. A floating contact-electric field gated tribotronic transistor (CGT) has been first proposed based on a SOI wafer and a mobile polytetrafluoroethylene (PTFE) layer (Fig. 4a), which can be gated by the contact and separation between the mobile layer and floating gate (Fig. 4b). The structure of the CGT is simpler and more

Please cite this article in press as: C. Zhang, Z.L. Wang, Tribotronics—A new field by coupling triboelectricity and semiconductor, Nano Today (2016), http://dx.doi.org/10.1016/j.nantod.2016.07.004

**Table 1**
Comparison of traditional FET, piezotronic transistor and CE-FET. Reprinted with permission from Ref. [67]. Copyright 2014 American Chemical Society.

| | Field effect transistor | Piezotronic transistor | CE-FET |
|---|---|---|---|
| Control: | External applied voltage controlling channel width | Self-generated inner piezopotential controlling interface/junction | Self-generated inner electrostatic potential controlling channel width |
| Structure: | 3-terminal (S, D, G) | 2-terminal | 2-terminal |
| Gate: | Voltage | Strain/mechanical deformation | Contact/Friction/Force/mechanical displacement |
| Sensing range: | None | Small | Large |
| Speed: | Fast (GHz) | Slower (KHz, MHz) | Slower (KHz, MHz) |
| Materials: | General semiconductor (Si, Ge . . .) | Piezoelectric semiconductor (ZnO, GaN . . .) | General semiconductor (Si, Ge . . .) |
| Applications: | Amplification, variable resistor, electronic switch | Human/environmental interfacing, sensors, MEMS, flexible electronics, piezotronics, piezophotonics, piezo-phototronics, piezotromagnetism | Human/environmental interfacing, sensors, MEMS, flexible electronics, tribotronics, tribophotonics, tribo-phototronics, tribotromagnetism |

practicable than the CE-FET for the mobile part is just a PTFE layer, without the metal layer and any connection to the electrodes. With this improvement, the PTFE layer can be considered as a "foreign" object, which has an effect as injecting charges on the floating gate when contact or separate. The contact-gated tribotronic logic device (CGL) is composed with two opposite CGTs (Fig. 4c), which can exhibit logic high level when the external force is applied and logic low level when the external force is released (Fig. 4d). With two integrated CGLs, the tribotronic NAND gate has been demonstrated and the operation results of two input forces accord well with the characteristics of the logic NAND operation and complementary metal-oxide-semiconductor (CMOS) logic level standard (Fig. 4e and f).

Similarly, other universal combinational logic circuits, including NOT, AND, OR, NOR, XOR and XNOR gates, have also been demonstrated for performing mechanical-electrical coupled tribotronic logic operations. Different from the conventional electrically-controlled logic units, the contact-gated tribotronic logic units have realized the direct interaction between the external environment and the silicon-based integrated circuits. The tribotronic circuits and operations could extend to further research on a new branch of tribotronic digital circuits, such as trigger, sequential logic circuit and memory, which are highly expected as a new technique for human-computer interaction.

*Organic tribotronic light emitting diode*

By coupling an organic thin film transistor (OTFT) and a TENG, the organic tribotronic transistor (OTT) has been developed, in which the charge carrier transport can be modulated by the contact induced electrostatic potential of the TENG instead of the traditional gate voltage. The OTFT has a MIS capacitor structure of indium tin oxide (ITO)/$Ta_2O_5$/pentacene, and the TENG has a structure of Cu/polyvinylchloride (PVC)/Cu in vertical contact-separation mode. By further integrating with an organic light-emitting diode (OLED) based on an *N*, *N*′-diphenyl- *N*, *N*′-bis(1,1′-biphenyl)-4,4′-diamine (NPB) film and a tris-(8-hydroxyquinoline) aluminum ($Alq_3$) film, the contact-electrification-gated light-emitting diode (CG-LED) has been fabricated [69] (Fig. 5a). The CG-LED is equivalent as the electrical connection of the OTT and OLED in series with a voltage source, in which applying a physical contact can modulate the

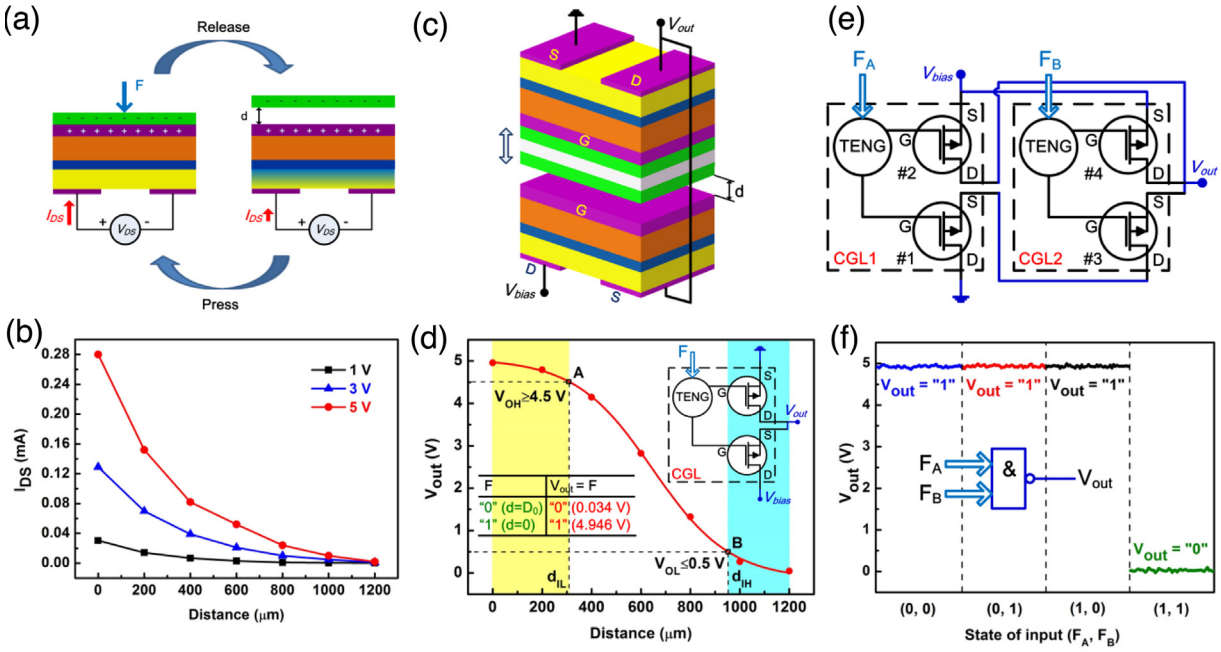


**Fig. 4.** Floating contact-electric-field gated tribotronic transistor (CGT) and contact-gated tribotronic logic device (CGL). (a) Working principle of the CGT with the applied and released external force. (b) $I_{DS}$-*d* characteristics of the CGT at different drain voltages. (c) Structure of the two opposite CGTs based CGL. (d) $V_{out}$-*d* transfer characteristic of the CGL. The output voltage in yellow region is the logic "1" output region, while in blue region is the logic "0" output region for the CGL with the CMOS level standard. The insets are the equivalent circuit and experimental truth table of the CGL. (e) Equivalent circuit of the two CGLs based NAND gate. (f) The output voltages of the NAND gate at different states of input forces. The inset is logic symbol of the tribotronic logic NAND gate. Reprinted with permission from Ref. [68]. Copyright 2015 John Wiley & Sons, Inc.

Please cite this article in press as: C. Zhang, Z.L. Wang, Tribotronics—A new field by coupling triboelectricity and semiconductor, Nano Today (2016), http://dx.doi.org/10.1016/j.nantod.2016.07.004

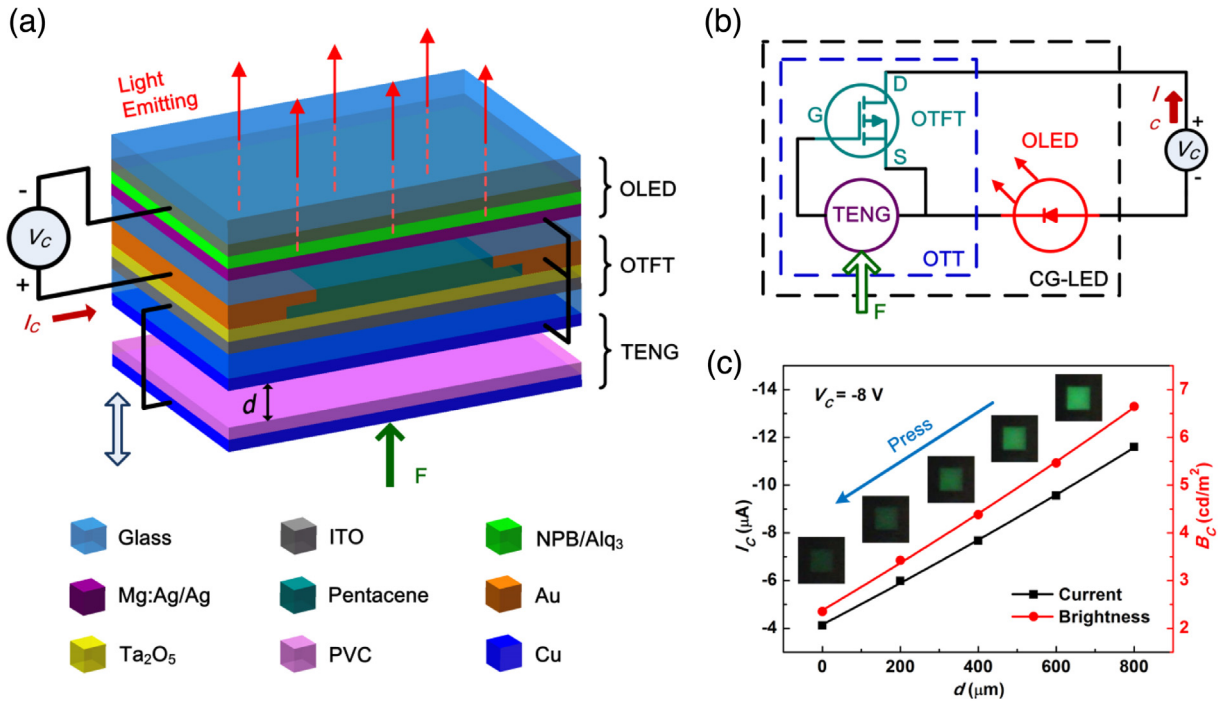


**Fig. 5.** Contact-electrification-gated light-emitting diode (CG-LED). (a) Schematic diagram of the CG-LED. (b) Equivalent circuit of the CG-LED. (c) Current and brightness transfer characteristics of the CG-LED. The insets show the light-emitting photographs from bright to dark when physically pressed. Reprinted with permission from Ref. [69]. Copyright 2015 John Wiley & Sons, Inc.

drain-source current in the OTT as well as the light-emission intensity of the OLED (Fig. 5b). Two modulation modes of the CG-LED by the applied physical contact are realized. One is press to darken. In this mode, when the CG-LED is pressed, the brightness nearly linearly decreases from 6.65 to 2.36 cd/m$^2$ at a supply voltage of −8 V (Fig. 5c). While the other is press to brighten. When the CG-LED is pressed, the brightness nearly linearly increases from 0.75 to 8.01 cd/m$^2$ at the same supply voltage.

Different from the conventional electrically-controlled organic light-emitting transistor (OLET), the CG-LED has realized the direct modulation of the electroluminescence device by the external environment/stimuli. As a new tribotronic functional device with only metal and organic materials, the CG-LED has first introduced optoelectronics into tribotronics, and opened up a new field of tribo-phototronics, which could have great prospects in mechanical imaging, interactive display, flexible/touch optoelectronics, and micro-opto-electro-mechanical systems (MOEMS).

*Flexible organic tribotronic transistor memory*

As the triboelectric potential of the TENG has been used to gate transistors, it can be employed for the transistor memory as well in place of the traditional gate voltage for programming, which can be an active memory device for external touch actions [70]. By coupling an organic transistor memory (OTM) and a TENG with flexible materials, the flexible organic tribotronic transistor memory (OTTM) has been proposed (Fig. 6a). The OTM has a structure of ITO/$Ta_2O_5$/polymethyl methacrylate (PMMA)/pentacene, with a separated Ta floating gate layer sandwiched between two PMMA layers. The TENG has a structure of Cu/PVC/Cu in vertical contact-separation mode. The writing and erasing of the signals in the OTTM can be realized by the contact electrification of the external physical touch. By further coupling with a flexible OLED with a structure of ITO/NPB/$Alq_3$/Mg:Ag/Ag, a visible and wearable touch monitoring system has been successfully developed. In the touch monitoring system, the TENG is a triggering input/reset unit for the external physical touch, the OTM is a storage unit for recording the detected triggering, and the OLED is a touch signal-output functional unit for the visual reading (Fig. 6b). This system can be used for monitoring the external touch and protecting confidential documents (Fig. 6c). After writing and erasing procedures by the external touch, the shift and return of the transfer curve have demonstrated great performances in stability and repeatability (Fig. 6d).

Unlike traditional OTMs programed by electric signals, the OTTM can be programed by the external mechanical touches without gate voltage supply, which has realized the direct interaction between the external environment and the memory. It has demonstrated the mechanical-electrical coupled tribotronic memory properties and great applications in intelligent control, security monitoring, functional instruments and wearable functional electronics.

*Tribotronic phototransistor*

The contact induced electrostatic potential of the TENG has been used to modulate the electroluminescence, which is also could be used to modulate the photoelectric conversion in the first proposed tribotronic phototransistor (TPT) [71]. On the basis of the CE-FET structure, a PN junction is formed in the p-type conduction channel layer by the heavy phosphorus ion implantation and rapid thermal annealing. The photocurrent can be generated from the PN junction by the illumination in place of the drain-source voltage in the CE-FET. As the contact and separation between the mobile fluorinated ethylene propylene (FEP) layer and the gate electrode, the charge carrier concentration in the p-type conduction channel layer could be regulated, which will induce the photocurrent modulation by the external contact. As an alternative design of the TPT, a coupled energy-harvester (CEH) has been fabricated, in which the periodical contact and separation between the FEP layer and electrodes are driven by the wind (Fig. 7a). The CEH can be equivalently considered as the integration of a photodiode, a MOSFET and a direct-current TENG, which is used for simultaneously scavenging solar and wind

Please cite this article in press as: C. Zhang, Z.L. Wang, Tribotronics—A new field by coupling triboelectricity and semiconductor, Nano Today (2016), http://dx.doi.org/10.1016/j.nantod.2016.07.004

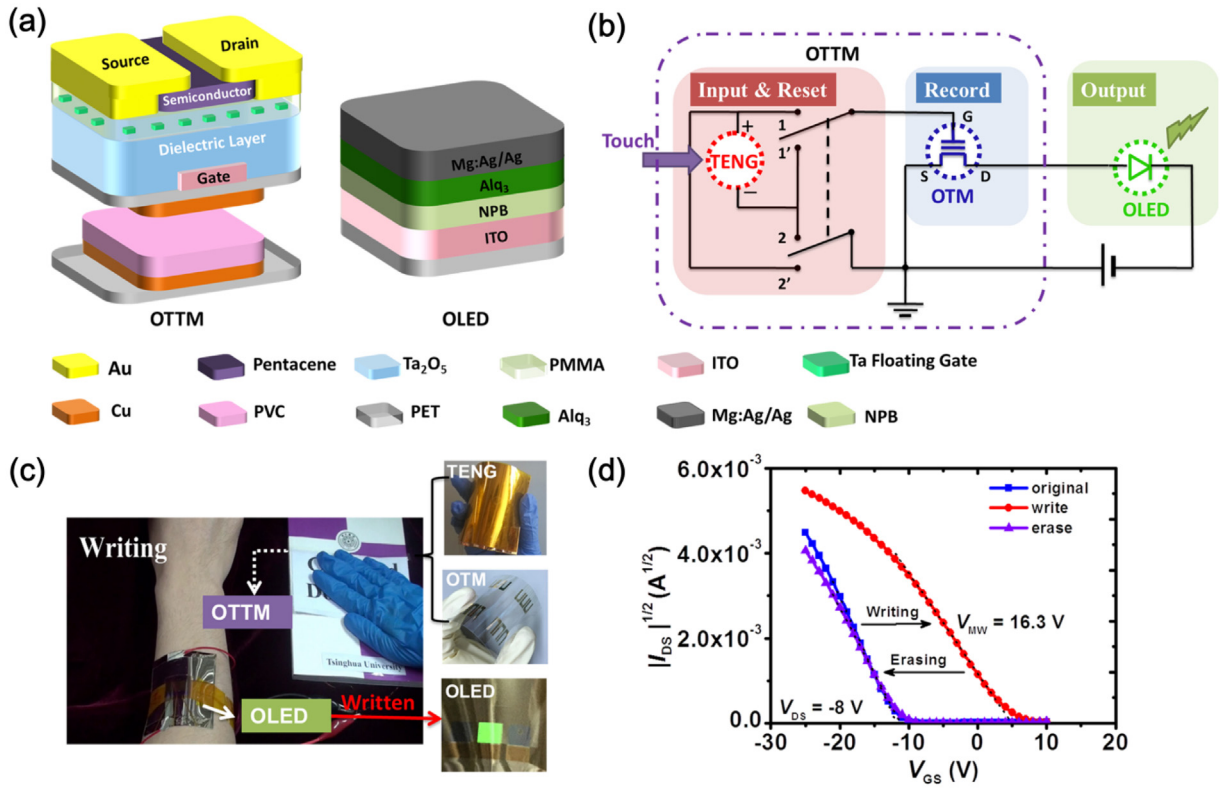


**Fig. 6.** Flexible organic tribotronic transistor memory (OTTM) for a visible and wearable touch monitoring system. (a) Schematic diagram of the OTTM and OLED. (b) Schematics of the touch monitoring system. (c) Photographs of the system for monitoring the external touch. (d) Shift and return of the transfer curve after writing and erasing procedures by external touch. Reprinted with permission from Ref. [70]. Copyright 2015 John Wiley & Sons, Inc.

energies (Fig. 7b). Moreover, the wind-induced output voltage on the external resistance is also used as the inner gate voltage of the TPT for modulating and enhancing the solar energy conversion. The measured characteristics of the CEH have shown that the short-circuit current, open-circuit voltage, and maximal output power have been greatly enhanced as the wind speed increases from 7 to 11 m/s at the sunlight intensity of 2 mW/cm$^2$ (Fig. 7c).

As new tribo-phototronic devices, the TPT has demonstrated the triboelectric-charge-enhanced photodetection and the CEH has established an effective coupling mechanism between different energy transducers for enhancing the hybrid energy harvesting. This work has further expanded the functionality of tribotronics in photodetection and energy harvesting, and demonstrated a potential way for efficiently harvesting and utilizing the multiple energy.

## Tribotronics of diversified materials

### *$MoS_2$ tribotronic tactile switch*

Besides the silicon-based and organic materials, the tribotronic devices have also been extended to a new two-dimensional (2D) material of $MoS_2$ to demonstrate the material diversification [72]. By coupling a single-electrode mode TENG and a $MoS_2$ field effect transistor, a $MoS_2$ tribotronic transistor has been developed (Fig. 8a). The single or few-layer $MoS_2$ flake was processed from bulk $MoS_2$ by the mechanical exfoliation method and directly transferred to the highly doped p-type silicon substrate with 300 nm thick $SiO_2$. The drain and source electrodes were prepared on $MoS_2$ flakes by ultraviolet lithography and successive evaporation of Cr

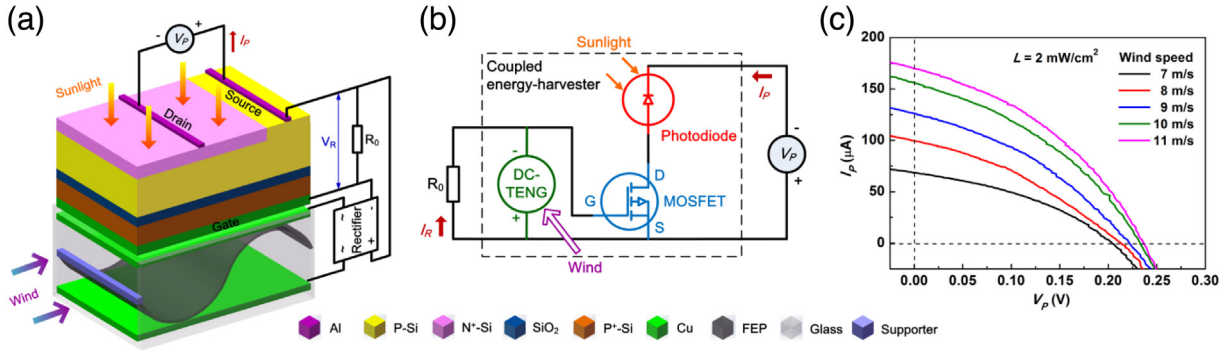


**Fig. 7.** Tribotronic phototransistor (TPT) as coupled energy-harvester (CEH) for simultaneously scavenging wind and solar energies. (a) Schematic diagram of the CEH. The harvested wind energy is used for gating the TPT and enhancing the solar energy conversion. (b) Equivalent circuit of the CEH, with the integration of a photodiode, a MOSFET and a direct-current TENG. (c) Enhanced $I_P$-$V_P$ characteristics for harvesting solar energy with increasing wind speed. Reprinted with permission from Ref. [71]. Copyright 2016 John Wiley & Sons, Inc.

Please cite this article in press as: C. Zhang, Z.L. Wang, Tribotronics—A new field by coupling triboelectricity and semiconductor, Nano Today (2016), http://dx.doi.org/10.1016/j.nantod.2016.07.004

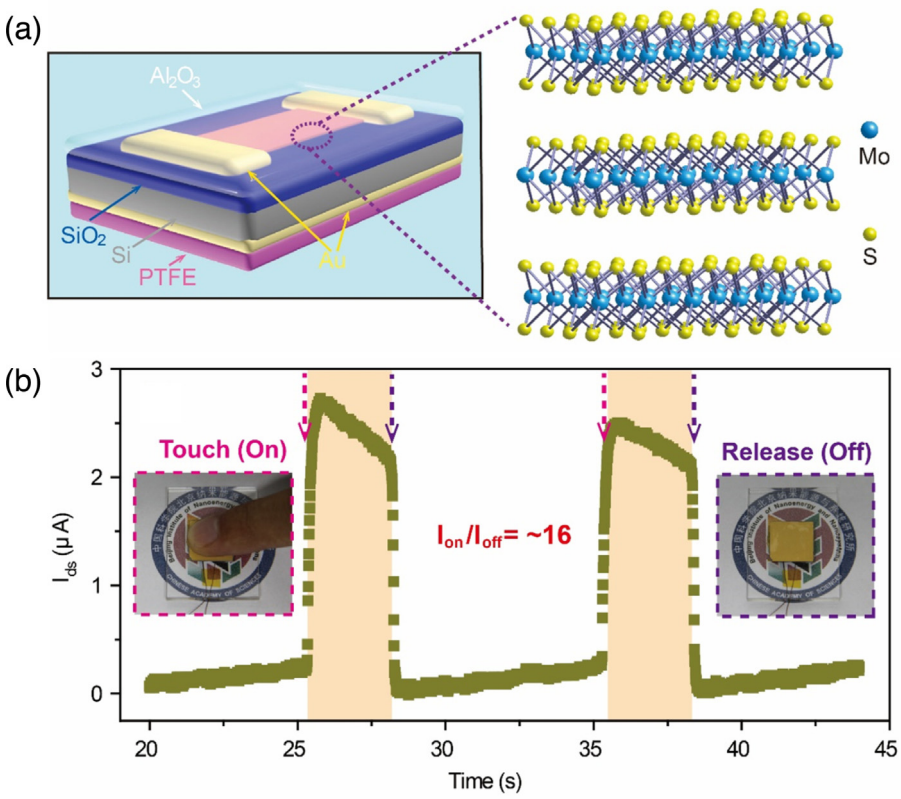


**Fig. 8.** $MoS_2$ tribotronic transistor as smart tactile switch. (a) Schematic diagram of the $MoS_2$ tribotronic transistor. The inset is the side-view of the three-layer $MoS_2$ crystal structure in the device. (b) Finger-triggered response of the $MoS_2$ tribotronic transistor as an active smart tactile switch. Reprinted with permission from Ref. [72]. Copyright 2016 John Wiley & Sons, Inc.

and Au. For a stable package of the device, a 30 nm thick $Al_2O_3$ layer was deposited on the top of the transistor by atomic layer deposition (ALD). A 50 nm thick Au film as a floating gate was deposited on the bottom surface of the silicon substrate with ohmic contact, and a PTFE film with a thickness of 25 μm and an area of 14 × 14 $mm^2$ was smoothly attached on the back. Once an external material contacts with or separates from the PTFE film, negative charges are induced by triboelectrification on the PTFE surface, which act as a "gate" voltage to modulate the carrier transport in the $MoS_2$ channel. The drain-source current can be tuned from 1.56 μA to 15.74 μA for nearly ten times enhancement. After about 1000 cycles test, the drain-source current with little hysteresis has shown the great stability and repeatability of the device.

The $MoS_2$ tribotronic transistor could be used as an active smart tactile switch for human-machine interfacing. When a finger touches the PTFE film, charge transfer results in positive charges on the finger while negative charges on the PTFE film and the on/off ratio of the device can reach as high as about 16 for switching LEDs (Fig. 8b). Moreover, the $MoS_2$ tribotronic transistor can also be widely applied as mechanical displacement sensors, visualized touch sensors, and smart skin. This work has extended the emerging tribotronics to 2D materials and demonstrated the material diversification of this new field, which may promote the development of tribotronics with new features.

### *$MoS_2$ tribotronic photodetector*

With the photoconductive property, $MoS_2$ could be used to develop the tribotronic phototransistor as well with the modulated and enhanced photoresponsivity [73]. By a conjunction of a $MoS_2$ phototransistor and a TENG in sliding mode, a $MoS_2$ tribotronic phototransistor is proposed for this purpose (Fig. 9a). Different from the structure of $MoS_2$ tribotronic transistor, the bottom friction layer consists of a 20 μm thick FEP film attached with a 50 μm thick Al foil as a free-sliding layer. By a relative sliding on the device, the induced positive charges on the back gate of the $MoS_2$ phototransistor act as a "gate" to increase the channel conductivity as the effect of traditional back gate voltage, and thus increase the responsivity of the photodetection. With the sliding distance of 8 mm, the photoresponsivity is drastically enhanced from 221.0 A/W to 727.8 A/W at the 10 mW/$cm^2$ ultraviolet excitation intensity and 1 V bias voltage (Fig. 9b).

The $MoS_2$ tribotronic phototransistor has demonstrated the stable characteristics as well (Fig. 9c), which could be used in optical sensing, imaging and photodetection. Unlike the silicon-based tribotronic phototransistor with PN junction, this work has demonstrated tribotronic enhanced photodetection with the tunable photoconductive property based on 2D material and provided a new method for actively adjustable photoelectric devices with high photoresponsivity via human interfacing.

### *InSb tribotronic force-pad*

All the tribotronic devices above are based on a TENG and a back-gate MOSFET. Although the back-gate electrode is completely off an external voltage supply, the fabrication process has not eliminated for the role of an electrode of the TENG. Different from the back-gate tribotronic transistors, a novel InSb tribotronic transistor on the flexible force-pad application has been developed based on a single-electrode mode TENG and a top-gate InSb FET [74]. The top-gate FET is fabricated on a flexible substrate with a structure of poly(ethylene oxide) (PEO)/InSb/polyethylene terephthalate (PET). The n-type InSb was used for a conduction channel and the PEO served as a dielectric layer. The Ag has an Ohmic contact with the

Please cite this article in press as: C. Zhang, Z.L. Wang, Tribotronics—A new field by coupling triboelectricity and semiconductor, Nano Today (2016), http://dx.doi.org/10.1016/j.nantod.2016.07.004

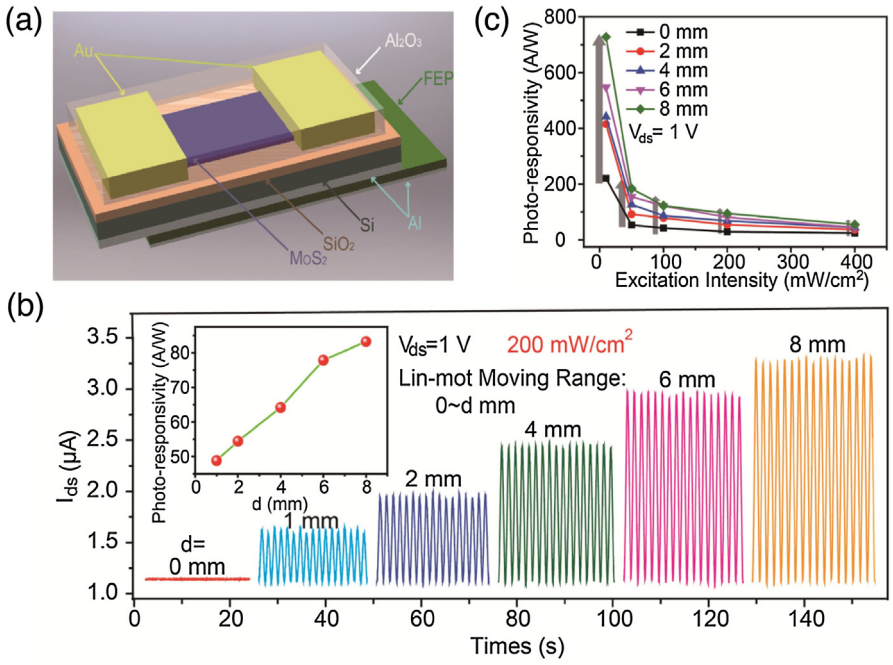


**Fig. 9.** $MoS_2$ tribotronic phototransistor as photodetector. (a) Schematic diagram of the $MoS_2$ tribotronic phototransistor based on a $MoS_2$ phototransistor and a sliding triboelectric nanogenerator. (b) $I_{ds}$ output characteristics at different sliding distances. The inset is photo-responsivity transfer characteristic. (c) Tribotronic enhanced photo-responsivity of the $MoS_2$ phototransistor at different excitation intensity and sliding distances. Reprinted with permission from Ref. [73]. Copyright 2016 John Wiley & Sons, Inc.

InSb as the drain and source electrodes. When the mobile PTFE layer contacts with the PEO for electrification, the PTFE surface has negative charges while the PEO surface has positive charges according to the triboelectric series. When the PTFE layer separates from the PEO, the positive charges on the PEO surface will induce the enhancement zone in the n-type InSb and thus increase the drain-source current (Fig. 10a). The $I_{DS}$-$V_{DS}$ output characteristics could be modulated with different separated distances (Fig. 10b), and the drain-source current progressively increases from 6 μA to 12 μA at a drain voltage of 1 V with different separated distances in the range of 0–80 μm (Fig. 10c).

Alternatively, the mobile layer could be an Al film for contact electrification with the PEO, resulting in that the Al has positive charges while the PEO surface has negative charges according to the triboelectric series. The negative charges on the PEO surface will induce the depletion zone in the n-type InSb and thus decrease the drain-source current from 7 μA to 1.5 μA at the same conditions. Therefore, the traditional top-gate electrode in the FET has been eliminated and replaced by an external mobile PTFE and an Al film, which could mechanically contact with the PEO surface to serve as a negative and positive gate voltage, respectively. The InSb tribotronic transistor as force-pad reported in this work keeps out of the top-gate electrode and the dielectric layer is served as a frictional layer of the TENG, which has further simplified the structure and fabrication process of tribotronic transistor.

## Theory of tribotronics

### *Theoretical study of tribotronic logic operation and mechanical sensing*

With the development of various tribotronic devices, a theoretical study is strongly desired as the theoretical foundation and optimization strategy for current and future tribotronics. By both analytical calculations and numerical simulations, the theory of tribotronics has basically established on both the logic operation and mechanical sensing [75].

As a basic tribotronic logic unit, the CMOS-based tribotronic inverter can be equivalent as the coupling of a TENG, an n-type MOSFET (NMOS) and a p-type MOSFET (PMOS) (Fig. 11a). When the TENG is working at quasi-steady state, the $V_{OUT}$ of the tribotronic inverter gradually changes as the output increases from 0 to above $V_{Gmax}$. According to the Kirchhoff's law and different working modes of the MOSFETs, there are five working regions for the tribotronic inverter [75]. Firstly, when the separation distance $x$ of the two surfaces in the TENG is in the range as:

$$x \le \frac{V_{TN}\varepsilon_0}{\sigma} \tag{2}$$

where $V_{TN}$ is the threshold voltage of the NMOS, $\sigma$ is the surface charge density of the polymer used in the TENG, and $\varepsilon_0$ is the permittivity of vacuum space. The NMOS is working at off mode, and the PMOS is working at linear mode. The $V_{OUT}$ of the tribotronic inverter is described as:

$$V_{OUT} = V_{DD} \tag{3}$$

Secondly, when

$$\frac{V_{TN}\varepsilon_0}{\sigma} < x < \frac{\left(\sqrt{\frac{K_P}{K_N}}(V_{DD} - V_{TP}) + V_{TN}\right)\varepsilon_0}{\left(1 + \sqrt{\frac{K_P}{K_N}}\right)\sigma} \tag{4}$$

where $V_{TP}$ is the threshold voltage of the NMOS, $K_P$ and $K_N$ are the ratio constants of the PMOS and NMOS. The NMOS is in saturated mode and the PMOS is in linear mode. In this region,

$$V_{OUT} = \frac{\sigma x}{\varepsilon_0} - V_{TP} + \sqrt{\left(V_{DD} - \frac{\sigma x}{\varepsilon_0} - V_{TP}\right)^2 - \frac{K_N}{K_P}\left(\frac{\sigma x}{\varepsilon_0} - V_{TN}\right)^2} \tag{5}$$

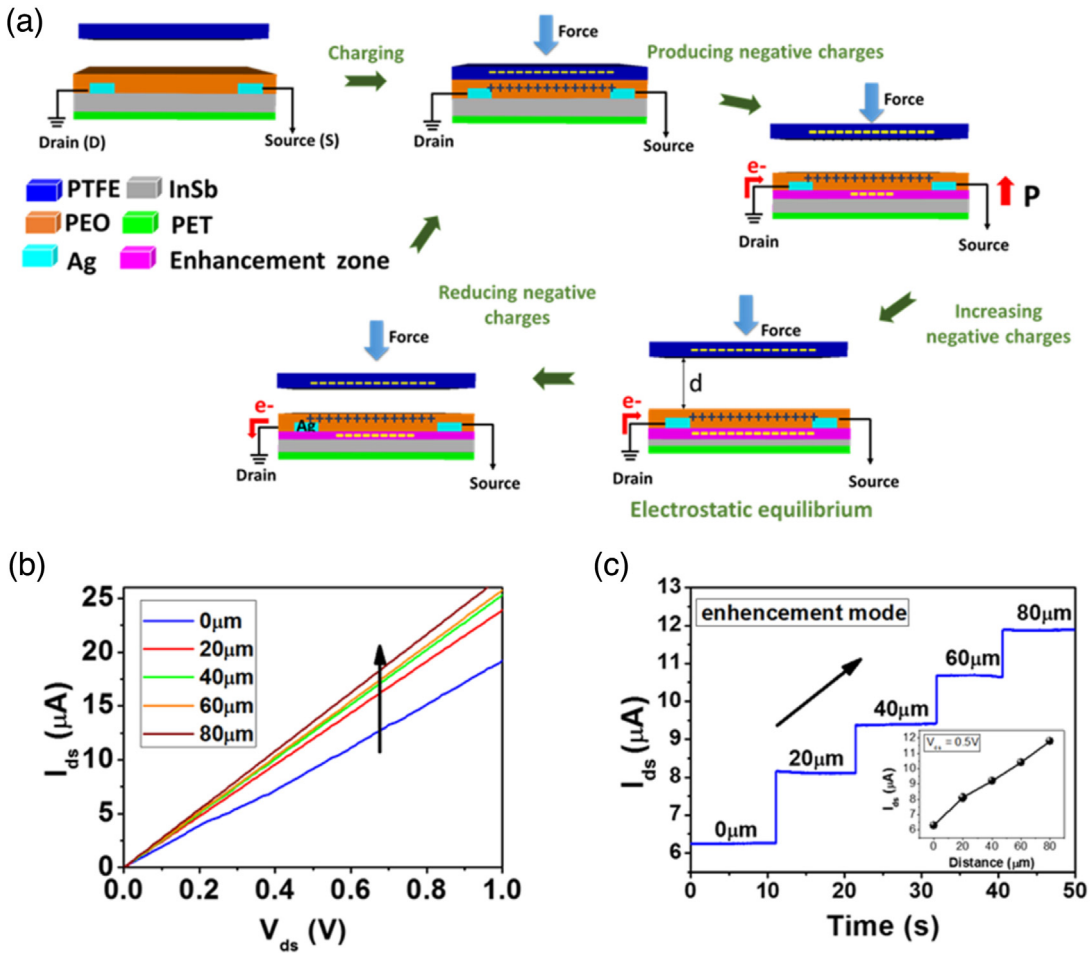


**Fig. 10.** InSb tribotronic transistor as force pad. (a) Working principle of the InSb tribotronic transistor with a mobile layer of the PTFE. (b) $I_{DS}$-$V_{DS}$ output characteristics with different separated distances. (c) $I_{DS}$ output characteristics at a drain voltage of 1 V with different separated distances in the range of 0–80 μm. The inset is $I_{DS}$-$d$ transfer characteristic. Reprinted with permission from Ref. [74]. Copyright 2016 Elsevier Ltd.

Thirdly, when

$$x = \frac{\left(\sqrt{\frac{K_P}{K_N}}(V_{DD} - V_{TP}) + V_{TN}\right)\varepsilon_0}{\left(1 + \sqrt{\frac{K_P}{K_N}}\right)\sigma} \tag{6}$$

the NMOS and PMOS are both in saturated mode, and

$$\frac{\sigma x}{\varepsilon_0} - V_{TN} + \sqrt{\left(\frac{\sigma x}{\varepsilon_0} - V_{TN}\right)^2 - \frac{K_P}{K_N}\left(V_{DD} - \frac{\sigma x}{\varepsilon_0} - V_{TP}\right)^2} < V_{OUT} < \frac{\sigma x}{\varepsilon_0} + V_{TP} + \sqrt{\left(V_{DD} - \frac{\sigma x}{\varepsilon_0} - V_{TP}\right)^2 - \frac{K_N}{K_P}\left(\frac{\sigma x}{\varepsilon_0} - V_{TN}\right)^2} \tag{7}$$

which means that $V_{OUT}$ will steeply decrease when $x$ passes this point. Fourthly, when

$$\frac{\left(\sqrt{\frac{K_P}{K_N}}(V_{DD} - V_{TP}) + V_{TN}\right)\varepsilon_0}{\left(1 + \sqrt{\frac{K_P}{K_N}}\right)\sigma} < x < \frac{(V_{DD} - V_{TP})\varepsilon_0}{\sigma} \tag{8}$$

the NMOS is in linear mode and the PMOS is in saturated mode. In this region,

$$V_{OUT} = \frac{\sigma x}{\varepsilon_0} - V_{TN} + \sqrt{\left(\frac{\sigma x}{\varepsilon_0} - V_{TN}\right)^2 - \frac{K_P}{K_N}\left(V_{DD} - \frac{\sigma x}{\varepsilon_0} - V_{TP}\right)^2} \tag{9}$$

Lastly, when

$$x \geq \frac{(V_{DD} - V_{TP})\varepsilon_0}{\sigma} \tag{10}$$

the NMOS is working at linear mode and the PMOS is at off mode. It can be described as:

$$V_{OUT} = 0 \tag{11}$$

By using the equations above, the behavior of the tribotronic inverter could be calculated with a set of parameters. The $V_{OUT}$ goes from "1" to "0" as $x$ goes up, and steeply inverts at the point of $x$ = 312 μm (Fig. 11b). The theoretical simulation has shown the CMOS-based tribotronic inverter is successfully realized and the results can be utilized as instruction for designing the right tribotronic logic devices.

The tribotronic device can be utilized as an effective mechanical sensor for the resistor loaded MOSFET is also commonly used as the small signal amplifier (Fig. 11c). In this circuit, $R_1$ and $R_2$ are used to provide a DC bias to the MOSFET. By Kirchhoff's law, the amplification gain $A_V$ can be described as [75]:

$$A_V = \sqrt{\frac{C_{TENG}(-(\omega C_{GD}R_L)^2 + (g_m R_L)^2)}{(C_{TENG} + C_{GS} + C_{GD}(g_m R_L + 1))^2 - (C_{TENG} + C_{GS})^2(\omega C_{GD}R_L)^2}} \tag{12}$$

Please cite this article in press as: C. Zhang, Z.L. Wang, Tribotronics—A new field by coupling triboelectricity and semiconductor, Nano Today (2016), http://dx.doi.org/10.1016/j.nantod.2016.07.004

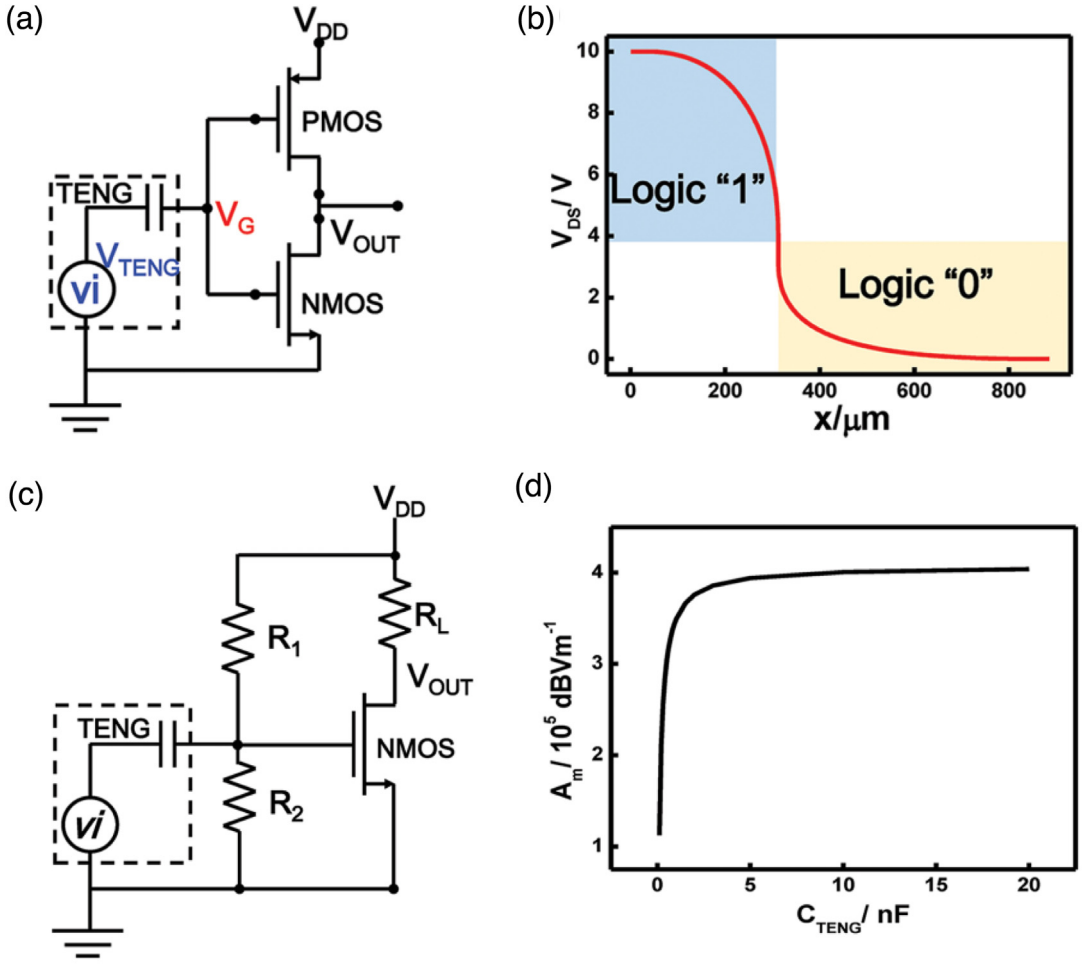


**Fig. 11.** Theoretical analysis of tribotronic devices on logic operation and mechanical sensing. (a) Circuit scheme of tribotronic device as a CMOS inverter gated by TENG. (b) Calculated behavior of the tribotronic inverter. The logic output goes from "1" to "0" as the displacement of TENG goes up. (c) Circuit scheme of tribotronic device as mechanical sensing. (d) Relationship between gain and TENG capacitance. The larger capacitance leads to the higher circuit gain. Reprinted with permission from Ref. [75]. Copyright 2015 John Wiley & Sons, Inc.

where $C_{TENG}$, $C_{GD}$ and $C_{GS}$ are the inherent capacitances of TENG and MOSFET, respectively, $g_m$ is the intrinsic transconductance of the MOSFET, and $\omega$ is the frequency of mechanical input. The mechanical sensitivity $A_m$ can be presented as [75]:

$$A_m = \frac{2\sigma A_V}{\varepsilon_0} \tag{13}$$

The relationship between $C_{TENG}$ and the maximum $A_m$ has been simulated when $C_{TENG}$ changes from 500 pF to 30 nF (Fig. 11d). The analytical calculation has shown the linear relationship stands when $C_{TENG}$ is small while the $A_m$ tends to saturate when $C_{TENG}$ increases to above 3 nF, which indicates larger TENG capacitance and higher surface charge density will lead to higher gain for the mechanical sensor. The simulation method and results have important significance for the gain optimization of tribotronics as the mechanical sensing.

*Theoretical study of tribotronic MOSFET performances*

By the finite element analysis (FEA) method, the performances of tribotronic MOSFET based on two fundamental working modes have been theoretically studied, which could provide in-depth understanding of physical mechanisms and design guidance for potential applications of tribotronics [76].

As a built model in the FEA, the tribotronic MOSFET is composed of a traditional NMOS and a 25 nm thick PTFE layer with aluminum electrode coated at its back as the mobile electrode (Fig. 12a). Equal triboelectric charges in opposite polarities are generated by contact electrification on the PTFE layer and gate electrode, respectively. When the distance $d$ increases to the threshold distance $d_{th}$, the triboelectric charges induced gate voltage reaches the threshold voltage $V_{th}$ and the NMOS turns on. The first working mode is that the mobile electrode is connected to the grounded source and bulk electrodes, while the second one is that the mobile electrode is isolated from all other electrodes as a "floating" one, which are defined as "w/feedback" and "w/o feedback", respectively. The conduction channel length $L$ is 1 μm and the distance $d$ between the PTFE layer and the gate electrode varies from 1 nm to 3 μm. With a set of parameters such as doping concentration, doping profile, and detailed geometrical dimension, the $I_{DS}$-$d$ characteristics at different $V_{DS}$ have been demonstrated (Fig. 12b). In the "w/o feedback" mode, $I_{DS}$ of the transistor increases gradually with $d$ (dash-dot lines), which operates as a general short-channel NMOS. While in the "w/feedback" mode, $I_{DS}$ of the transistor first increases quickly and gradually reaches a saturation (solid lines), which can be used as an electromechanical switch with quick switching between "on" and "off" states by separating the PTFE layer from gate electrodes for a short distance of hundreds of nanometers.

Please cite this article in press as: C. Zhang, Z.L. Wang, Tribotronics—A new field by coupling triboelectricity and semiconductor, Nano Today (2016), http://dx.doi.org/10.1016/j.nantod.2016.07.004

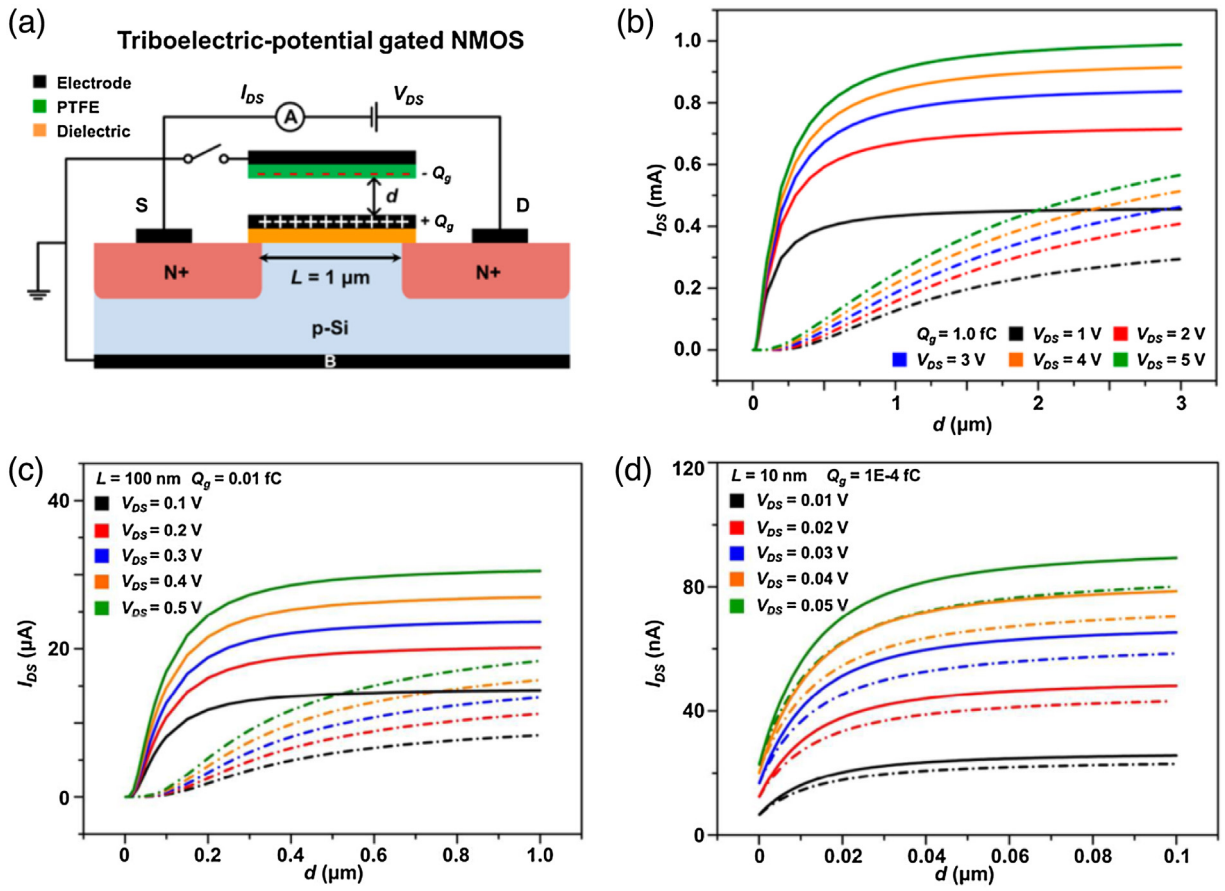


**Fig. 12.** Theoretical analysis on the performances of tribotronic MOSFET. (a) Schematic illustration of tribotronic NMOS, which is composed of a traditional silicon-based NMOS and a PTFE layer with aluminum electrode coated at its back as mobile electrode. (b) $I_{DS}$-$d$ characteristics of tribotronic NMOS with conduction channel length $L$ of 1 μm and triboelectric charges on gate electrode $Q_g$ of 1.0 fC under different $V_{DS}$ biases from 1 to 5 V. (c) $I_{DS}$-$d$ characteristics of tribotronic NMOS with $L$ of 100 nm and $Q_g$ of 0.01 fC under different $V_{DS}$ biases from 0.1 to 0.5 V. (d) $I_{DS}$-$d$ characteristics of tribotronic NMOS with $L$ of 10 nm and $Q_g$ of $10^{-4}$ fC under different $V_{DS}$ biases from 0.01 to 0.05 V. Reprinted with permission from Ref. [76]. Copyright 2016 American Chemical Society.

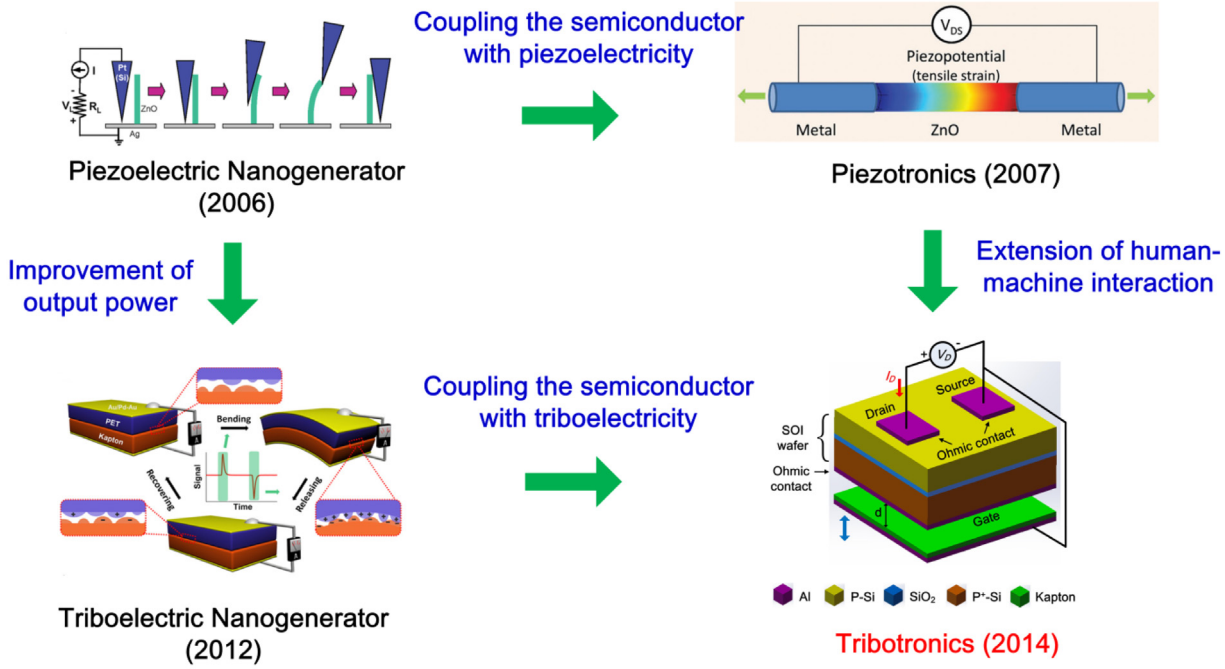


**Fig. 13.** Evolution of some main ideas in the past ten years in the field. As an extension of the proposed nanogenerator in 2006, piezotronics in 2007 and triboelectric nanogenerator in 2012, tribotronics is another original and novel field in the development of nano-energy and nano-electronics. Reprinted with permission from Ref. [6]. Copyright 2006 The American Association for the Advancement of Science. Reprinted with permission from Ref. [20]. Copyright 2013 American Chemical Society. Reprinted with permission from Ref. [26]. Copyright 2012 Elsevier Ltd. Reprinted with permission from Ref. [67]. Copyright 2014 American Chemical Society.

Please cite this article in press as: C. Zhang, Z.L. Wang, Tribotronics—A new field by coupling triboelectricity and semiconductor, Nano Today (2016), http://dx.doi.org/10.1016/j.nantod.2016.07.004

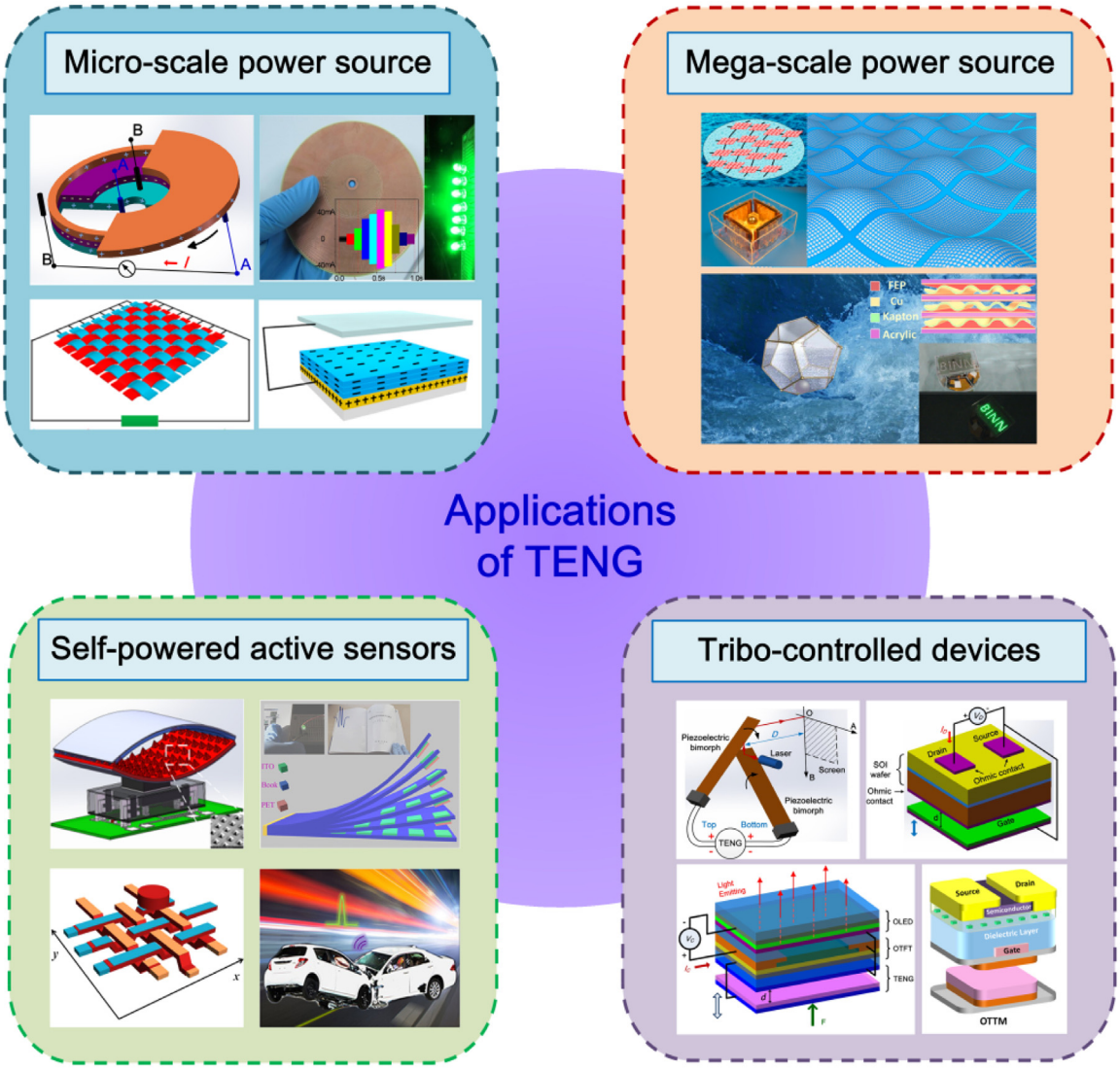


**Fig. 14.** Four applications of TENG. Besides the micro-scale power source, mega-scale power source and self-powered sensors, tribotronics is a new application of TENG as triboelectric-voltage-controlled (tribo-controlled) devices. Reprinted with permission from Refs. [35,77]. Copyright 2014 John Wiley & Sons, Inc. Reprinted with permission from Refs. [36]. Copyright 2015 Springer. Reprinted with permission from Refs. [37,67]. Copyright 2014 American Chemical Society. Reprinted with permission from Ref. [38]. Copyright 2016 Springer. Reprinted with permission from Refs. [49,57]. Copyright 2015 American Chemical Society. Reprinted with permission from Ref. [50]. Copyright 2016 Elsevier Ltd. Reprinted with permission from Ref. [54]. Copyright 2014 IOP Publishing Ltd. Reprinted with permission from Ref. [55]. Copyright 2014 Springer. Reprinted with permission from Ref. [56]. Copyright 2014 Elsevier Ltd. Reprinted with permission from Refs. [69,70]. Copyright 2015 John Wiley & Sons, Inc.

By scaling down conduction channel length $L$ of the NMOS in the model to 100 nm, 20 nm and 10 nm, respectively, all the relevant parameters of NMOS also scale down proportionally, whereas the thickness of PTFE layer and the generated triboelectric surface charge density keep unchanged considering that the contact electrification process remains the same. The simulation results show that when $L$ is much larger than the thickness of PTFE layer, the two working modes of tribotronic MOSFET show different characteristics and can be utilized in different applications. While when $L$ is smaller than the thickness of PTFE layer, the fast charge transfer process between mobile electrode and other electrodes in the "w/feedback" mode transit to a slow process and the two working modes are almost the same. The theoretical analyses have shown a great potential of tribotronics in large-scale array integration and applications in fingerprint recognition, wearable electronics, and so on.

## Summary and perspectives

In this review, the establishment and latest progress in tribotronics are systematically summarized. By applying on a common MIS capacitor in microelectronics, the TENG has been coupled with traditional MOSFET as a novel CE-FET for replacing the traditional gate voltage by external contact, which has established a direct interaction mechanism between the external environment and electronics. As a fundamental component, the CE-FET has derived a series of interactive functional devices and opened up a new field of tribotronics, which is about the devices fabricated using the electrostatic potential created by triboelectrification as a "gate" voltage to tune/control electrical transport and transformation in semiconductors for human-machine interaction. Various tribotronic functional devices have been developed with many potential applications. The tribotronic logic circuits have performed mechanical-electrical coupled tribotronic logic operations. The tribotronic LED has shown the contact electrification

Please cite this article in press as: C. Zhang, Z.L. Wang, Tribotronics—A new field by coupling triboelectricity and semiconductor, Nano Today (2016), http://dx.doi.org/10.1016/j.nantod.2016.07.004

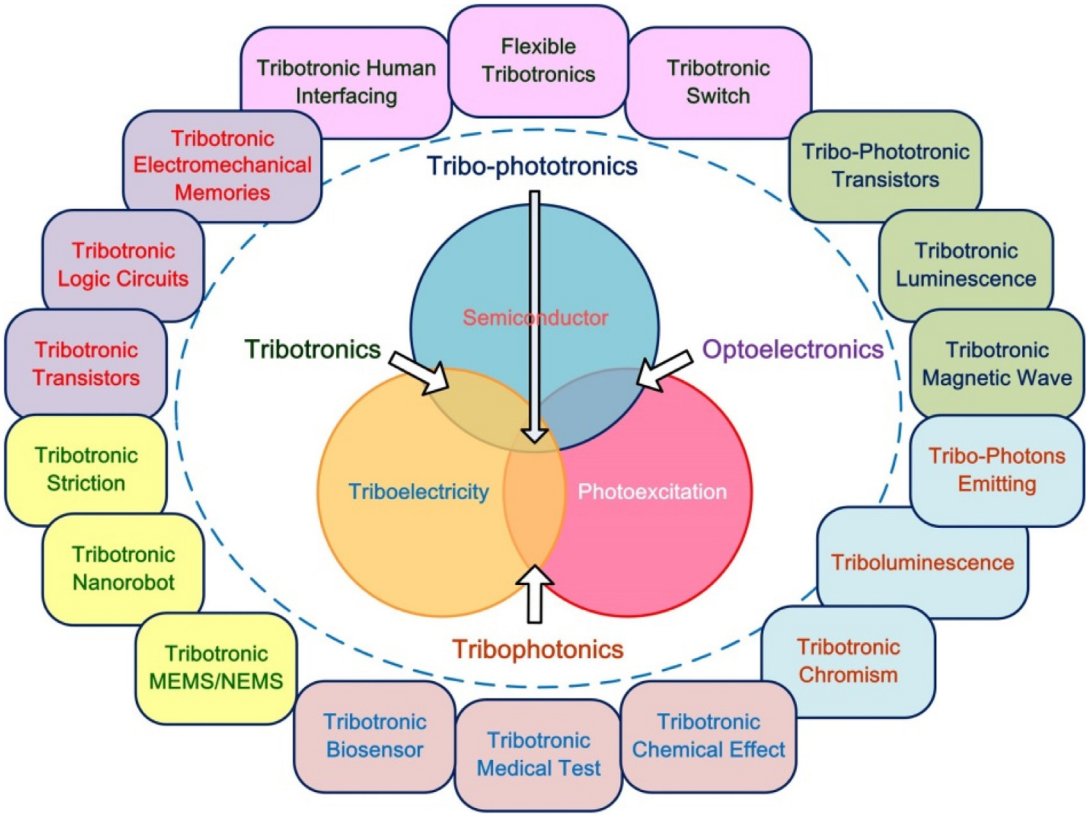


**Fig. 15.** Three-way coupling among triboelectricity, semiconductor, and photoexcitation, which can derive new fields of tribotronics, tribophotonics and tribophototronics. Plenty of potential directions and important applications are projected and expected to be explored in the near future. Reprinted with permission from Ref. [67]. Copyright 2014 American Chemical Society.

modulated electroluminescence. The tribotronic transistor memory has realized an active memory that can be written and erased by externally applied touch actions. The tribotronic phototransistor has demonstrated the triboelectric charges enhanced photoelectric conversion and hybrid energy harvesting. The silicon-based, flexible organic, $MoS_2$, InSb, and many other materials-based tribotronic devices have exhibited the material variety of tribotronics. The analytical calculations, numerical simulations and FEA of some tribotronic functional devices and their performances are also summarized by scaling down conduction channel length from 1 μm to 10 nm, which have shown a great potential of tribotronics in large-scale array integration.

Fig. 13 summarizes the evolution of some main ideas in the past ten years in the field. In 2006, the nanogenerator is first invented with piezoelectric semiconductor material for converting mechanical energy into electricity in nano-scale. By coupling the piezoelectricity with semiconductor, piezotronics is first proposed in 2007 for using the piezopotential as a "gate" voltage to tune/control charge carrier transport at a contact or junction. Since 2012, the TENG is first invented based on contact electrification and electrostatic induction with improved output power. By coupling the triboelectricity with semiconductor, tribotronics is first proposed as another original and novel field in 2014. Similar to piezotronics, tribotronics has self-generated inner controlling signal by external mechanical energy for active human-machine interaction, and also provided an active sensing method different from the conventional passive sensors [77,78]. More advantage than piezotronics, tribotronics has been considered to have a larger sensing range for the external environment, far more choice of materials, and wider application prospects in conjunction with the conventional semiconductor devices with the merits of TENG. Furthermore, the piezotronics are stimulated by the mechanical strain while the tribotronics can be gated by physical contact and mechanical displacement, which makes the tribotronics has greater durability with less fatigue accumulation in interaction with the external environment. Tribotronics is an extension of piezotronics, which could both lay important foundations for the development of human-machine interaction technology, and have important applications in sensors, intelligent interfacing, MEMS/NEMS, nanorobotics, and active flexible electronics. The current approach of using stretchable wires or interconnects for fabricating flexible electronics avoid any shape induced disturbance to the operation of the devices, while keep the entire structure can be bendable/strachable. In contrast, the active flexible electronics purposely use the deformation/strain introduced in the device for creating new functions, such as piezotronics and tribotronics. Such fields remain to be extensively studied in order to derive a new field of active flexible electronics.

Fig. 14 summarizes and exhibits the four different applications of TENG, in which tribotronics is also a new application of TENG. In the beginning, the TENG is used as a power source for micro and small electronics. With the rapid enhancement in output power and expected network distribution, it has demonstrated enormous potential for general power application at mega-scale. Moreover, it can be used as a self-powered active sensor for sensing a dynamic mechanical action without power supply. In these applications, power can be generated as long as there is a motion. And now in tribotronics, the TENG is used as a control source by taking advantage of the output voltage for modulating electronics, which can be a new application for triboelectric-voltage-controlled (tribo-

Please cite this article in press as: C. Zhang, Z.L. Wang, Tribotronics—A new field by coupling triboelectricity and semiconductor, Nano Today (2016), http://dx.doi.org/10.1016/j.nantod.2016.07.004

controlled) devices. It is expecting that future electronics can be actively controlled as long as touched!

By further introducing optoelectronics, Fig. 15 has schematically shown the three-way coupling among triboelectricity, semiconductor, and photoexcitation, which could consequently derive several new fields such as tribophotonics, tribo-phototronics, and tribo-electromagnetism for further research [75]. Looking forward to the development and future applications, tribotronics as a new emerging field has faced a series of challenges in theory mechanism, material selection, prototype device and practicability. More research work should be focused for seeking potential technical route as follows.

Firstly, establishing the fundamental theory of tribotronics. Based on nano-tribology and semiconductor device physics, the fundamental theory of tribotronics has to be further developed and the coupling mechanism of triboelectricity and semiconductor needs to be investigated in details. More fundamental theories are expected to establish for the fabrication and application of tribotronics.

Secondly, extending the material system of tribotronics. Based on the organic, nano-scale, and other new materials, the material diversification could be further exhibited, such as flexible, transparent and stretchable tribotronics, for the development of applications in human-machine interfacing, electronic skin, intelligent sensing, wearable devices, etc.

Thirdly, developing the functional devices of tribotronics. Based on optoelectronics, electromagnetism, MEMS/NEMS, integrated circuits, and other technologies, new branches of tribotronics are expected to explore and various novel functional tribotronic devices are highly desirable, such as tribotronic photoluminescence, tribotronic electromagnetic emission, tribotronic sequential logic circuits, tribotronic MEMS/NEMS, etc.

Lastly, integrating into the array devices of tribotronics. Based on the system integration technology, the functional tribotronic devices could be integrated and packaged in array, for developing the large-scale integrated tribotronic array devices, highly compact MEMS/NEMS, and large-area human-machine interactive interface.

As a new field by coupling triboelectricity and semiconductor, tribotronics has extended the emerging fields of nano-energy and nano-electronics with potential applications and significant impact. It will be a collaborative developing field with various disciplines such as material, mechatronics, information, automation, environment, energy, chemistry, biomedicine, and so on.

## Acknowledgements

The authors thank the support of National Natural Science Foundation of China (Nos. 51475099 and 51432005), Beijing Natural Science Foundation (Nos. 4163077), the “thousands talents” program for the pioneer researcher and his innovation team, China, and the Youth Innovation Promotion Association, CAS. We sincerely thank the following collaborators who made significant contributions to the work presented here: (not in particular order): Wei Tang, Chang Bao Han, Limin Zhang, Yaokun Pang, Fei Xue, Libo Chen, Tao Zhou, Xiang Yang, Guifang Dong, Liduo Wang, Lian Duan, Jing Li, Zhaohua Zhang, Ying Liu, Simiao Liu, Wenbo Peng, Ruomeng Yu and many others.

## References

[1] Z.L. Wang, Piezotronics and Piezo-Phototronics, Springer, Berlin, Heidelberg, 2013.
[2] T. Someya, T. Sekitani, S. Iba, Y. Kato, H. Kawaguchi, T. Sakurai, Proc. Natl. Acad. Sci. U. S. A. 101 (2004) 9966–9970.
[3] T. Someya, Y. Kato, T. Sekitani, S. Iba, Y. Noguchi, Y. Murase, H. Kawaguchi, T. Sakurai, Proc. Natl. Acad. Sci. U. S. A. 102 (2005) 12321–12325.
[4] Z.L. Wang, Nanogenerators for Self-Powered Devices and Systems, Georgia Institute of Technology SMARTech digital repository, 2011.
[5] Z.L. Wang, ACS Nano 7 (2013) 9533–9557.
[6] Z.L. Wang, J. Song, Science 312 (2006) 242–246.
[7] Z.L. Wang, Adv. Mater. 19 (2007) 889–892.
[8] Z.L. Wang, Adv. Mater. 24 (2012) 4632–4646.
[9] X. Wen, W. Wu, Y. Ding, Z.L. Wang, Adv. Mater. 25 (2013) 3371–3379.
[10] W. Wu, C. Pan, Y. Zhang, X. Wen, Z.L. Wang, Nano Today 8 (2013) 619–642.
[11] X. Wang, Am. Ceram. Soc. Bull. 92 (2013) 18–23.
[12] Z.L. Wang, W. Wu, Natl. Sci. Rev. 1 (2014) 62–90.
[13] Z.L. Wang, Mater. Sci. Eng. R Rep. 64 (2009) 33–71.
[14] Z.L. Wang, J. Phys. Chem. Lett. 1 (2010) 1388–1393.
[15] Y. Hu, Y. Chang, P. Fei, R.L. Snyder, Z.L. Wang, ACS Nano 4 (2010) 1234–1240.
[16] J. Zhou, Y. Gu, P. Fei, W. Mai, Y. Gao, R. Yang, G. Bao, Z.L. Wang, Nano Lett. 8 (2008) 3035–3040.
[17] W. Wu, Y. Wei, Z.L. Wang, Adv. Mater. 22 (2010) 4711–4715.
[18] W. Wu, Z.L. Wang, Nano Lett. 11 (2011) 2779–2785.
[19] S. Niu, Y. Hu, X. Wen, Y. Zhou, F. Zhang, L. Lin, S. Wang, Z.L. Wang, Adv. Mater. 25 (2013) 3701–3706.
[20] R. Yu, W. Wu, Y. Ding, Z.L. Wang, ACS Nano 7 (2013) 6403–6409.
[21] W. Wu, X. Wen, Z.L. Wang, Science 340 (2013) 952–957.
[22] Y. Hu, Y. Zhang, L. Lin, Y. Ding, G. Zhu, Z.L. Wang, Nano Lett. 12 (2012) 3851–3856.
[23] C. Pan, L. Dong, G. Zhu, S. Niu, R. Yu, Q. Yang, Y. Liu, Z.L. Wang, Nat. Photon. 7 (2013) 752–758.
[24] Q. Yang, Y. Liu, C. Pan, J. Chen, X. Wen, Z.L. Wang, Nano Lett. 13 (2013) 607–613.
[25] F. Xue, L.M. Zhang, W. Tang, C. Zhang, W.M. Du, Z.L. Wang, ACS Appl. Mater. Interf. 6 (2014) 5955–5961.
[26] F.R. Fan, Z.Q. Tian, Z.L. Wang, Nano Energy 1 (2012) 328–334.
[27] G. Zhu, C.F. Pan, W.X. Guo, C.Y. Chen, Y.S. Zhou, R.M. Yu, Z.L. Wang, Nano Lett. 12 (2012) 4960–4965.
[28] X.S. Zhang, M.D. Han, R.X. Wang, F.Y. Zhu, Z.H. Li, W. Wang, H.X. Zhang, Nano Lett. 13 (2013) 1168–1172.
[29] J.W. Zhong, Q.Z. Zhong, F.R. Fan, Y. Zhang, S.H. Wang, B. Hu, Z.L. Wang, J. Zhou, Nano Energy 2 (2013) 491–497.
[30] T.C. Hou, Y. Yang, H.L. Zhang, J. Chen, L.J. Chen, Z.L. Wang, Nano Energy 2 (2013) 856–862.
[31] P. Bai, G. Zhu, Z.H. Lin, Q.S. Jing, J. Chen, G. Zhang, J.S. Ma, Z.L. Wang, ACS Nano 7 (2013) 3713–3719.
[32] W. Tang, T. Jiang, F.R. Fan, A.F. Yu, C. Zhang, X. Cao, Z.L. Wang, Adv. Funct. Mater. 25 (2015) 3718–3725.
[33] W. Tang, C.B. Han, C. Zhang, Z.L. Wang, Nano Energy 9 (2014) 121–127.
[34] X. Pu, M. Liu, L. Li, C. Zhang, Y. Pang, C. Jiang, L. Shao, W. Hu, Z.L. Wang, Adv. Sci. 3 (2016) 1500255.
[35] C. Zhang, T. Zhou, W. Tang, C.B. Han, L.M. Zhang, Z.L. Wang, Adv. Energy Mater. 4 (2014) 1301798.
[36] C.B. Han, C. Zhang, W. Tang, X.H. Li, Z.L. Wang, Nano Res. 8 (2015) 722–730.
[37] T. Zhou, C. Zhang, C.B. Han, F.R. Fan, W. Tang, Z.L. Wang, ACS Appl. Mater. Interfaces 6 (2014) 14695–14701.
[38] T. Zhou, L.M. Zhang, F. Xue, W. Tang, C. Zhang, Z.L. Wang, Nano Res. 9 (2016) 1442–1451.
[39] W.Q. Yang, J. Chen, G. Zhu, J. Yang, P. Bai, Y.J. Su, Q.S. Jing, Z.L. Wang, ACS Nano 7 (2013) 11317–11324.
[40] S. Kim, M.K. Gupta, K.Y. Lee, A. Sohn, T.Y. Kim, K.S. Shin, D. Kim, S.K. Kim, K.H. Lee, H.J. Shin, D.W. Kim, S.W. Kim, Adv. Mater. 26 (2014) 3918–3925.
[41] C.B. Han, W.M. Du, C. Zhang, W. Tang, L.M. Zhang, Z.L. Wang, Nano Energy 6 (2014) 59–65.
[42] W. Tang, C. Zhang, C.B. Han, Z.L. Wang, Adv. Funct. Mater. 24 (2014) 6684–6690.
[43] G. Zhu, J. Chen, T.J. Zhang, Q.S. Jing, Z.L. Wang, Nat. Commun. 5 (2014) 3426.
[44] Z.H. Lin, G. Cheng, L. Lin, S. Lee, Z.L. Wang, Angew. Chem. Int. Ed. 52 (2013) 12545–12549.
[45] Z.H. Lin, G. Cheng, S. Lee, Z.L. Wang, Adv. Mater. 26 (2014) 4690–4696.
[46] G. Zhu, Y.J. Su, P. Bai, J. Chen, Q.S. Jing, W.Q. Yang, Z.L. Wang, ACS Nano 8 (2014) 6031–6037.
[47] X.N. Wen, W.Q. Yang, Q.S. Jing, Z.L. Wang, ACS Nano 8 (2014) 7405–7412.
[48] T. Jiang, L.M. Zhang, X. Chen, C.B. Han, W. Tang, C. Zhang, L. Xu, Z.L. Wang, ACS Nano 9 (2015) 12562–12572.
[49] J. Chen, J. Yang, Z. Li, X. Fan, Y. Zi, Q. Jing, H. Guo, Z. Wen, K.C. Pradel, S. Niu, Z.L. Wang, ACS Nano 9 (2015) 3324–3331.
[50] L.M. Zhang, C.B. Han, T. Jiang, T. Zhou, X.H. Li, C. Zhang, Z.L. Wang, Nano Energy 22 (2016) 87–94.
[51] Y. Yang, H.L. Zhang, Z.H. Lin, Y.S. Zhou, Q.S. Jing, Y.J. Su, J. Yang, J. Chen, C.G. Hu, Z.L. Wang, ACS Nano 7 (2013) 9213–9222.
[52] X.H. Li, C.B. Han, T. Jiang, C. Zhang, Z.L. Wang, Nanotechnology 27 (2016) 085401.
[53] Q.S. Jing, G. Zhu, W.Z. Wu, P. Bai, Y.N. Xie, R.P.S. Han, Z.L. Wang, Nano Energy 10 (2014) 305–312.
[54] W. Tang, T. Zhou, C. Zhang, C.B. Han, Z.L. Wang, Nanotechnology 25 (2014) 225402.
[55] L.M. Zhang, F. Xue, W.M. Du, C.B. Han, C. Zhang, Z.L. Wang, Nano Res. 7 (2014) 1215–1223.
[56] C.B. Han, C. Zhang, X.H. Li, L.M. Zhang, T. Zhou, W.G. Hu, Z.L. Wang, Nano Energy 9 (2014) 325–333.

Please cite this article in press as: C. Zhang, Z.L. Wang, Tribotronics—A new field by coupling triboelectricity and semiconductor, Nano Today (2016), http://dx.doi.org/10.1016/j.nantod.2016.07.004

[57] Y.K. Pang, X.H. Li, M.X. Chen, C.B. Han, C. Zhang, Z.L. Wang, ACS Appl. Mater. Interfaces 7 (2015) 19076–19082.
[58] C. Zhang, W. Tang, C.B. Han, F.R. Fan, Z.L. Wang, Adv. Mater. 26 (2014) 3580–3591.
[59] F.R. Fan, W. Tang, Y. Yao, J.J. Luo, C. Zhang, Z.L. Wang, Nanotechnology 25 (2014) 135402.
[60] C. Zhang, W. Tang, Y. Pang, C.B. Han, Z.L. Wang, Adv. Mater. 27 (2015) 719–726.
[61] C.B. Han, C. Zhang, J.J. Tian, X.H. Li, L.M. Zhang, Z. Li, Z.L. Wang, Nano Res. 8 (2015) 219–226.
[62] C.B. Han, T. Jiang, C. Zhang, X.H. Li, C.Y. Zhang, X. Cao, Z.L. Wang, ACS Nano 9 (2015) 12552–12561.
[63] J.H. Ahn, H.S. Kim, K.J. Lee, S. Jeon, S.J. Kang, Y. Sun, R.G. Nuzzo, J.A. Rogers, Science 314 (2006) 1754–1757.
[64] A. Javey, S. Nam, R.S. Friedman, H. Yan, C.M. Lieber, Nano Lett. 7 (2007) 773–777.
[65] S. Nam, X. Jiang, Q. Xiong, D. Ham, C.M. Lieber, Proc. Natl. Acad. Sci. U. S. A 106 (2009) 21035–21038.
[66] T. Bryllert, L.E. Wernersson, L.E. Froberg, L. Samuelson, IEEE Electron Device Lett. 27 (2006) 323–325.
[67] C. Zhang, W. Tang, L.M. Zhang, C.B. Han, Z.L. Wang, A.C.S. Nano, (2014) 8702–8709.
[68] C. Zhang, L.M. Zhang, W. Tang, C.B. Han, Z.L. Wang, Adv. Mater. 27 (2015) 3533–3540.
[69] C. Zhang, J. Li, C.B. Han, L.M. Zhang, X.Y. Chen, L.D. Wang, G.F. Dong, Z.L. Wang, Adv. Funct. Mater. 25 (2015) 5625–5632.
[70] J. Li, C. Zhang, L. Duan, L.M. Zhang, L.D. Wang, G.F. Dong, Z.L. Wang, Adv. Mater. 28 (2016) 106–110.
[71] C. Zhang, Z.H. Zhang, X. Yang, T. Zhou, C.B. Han, Z.L. Wang, Adv. Funct. Mater. 26 (2016) 2554–2560.
[72] F. Xue, L.B. Chen, L.F. Wang, Y.K. Pang, J. Chen, C. Zhang, Z.L. Wang, Adv. Funct. Mater. 26 (2016) 2104–2109.
[73] Y.K. Pang, F. Xue, L.F. Wang, J. Chen, J.J. Luo, T. Jiang, C. Zhang, Z.L. Wang, Adv. Sci. 3 (2016) 1500419.
[74] J.M. Wu, Y.H. Lin, B.Z. Yang, Nano Energy 22 (2016) 468–474.
[75] Y. Liu, S. Niu, Z.L. Wang, Adv. Electron. Mater. 1 (2015) 1500124.
[76] W. Peng, R. Yu, Y. He, Z.L. Wang, ACS Nano 10 (2016) 4395–4402.
[77] Y. Zang, F. Zhang, D. Huang, X. Gao, C. Di, D. Zhu, Nat. Commun. 6 (2015) 6269.
[78] P. Ray, V.R. Rao, Appl. Phys. Lett. 102 (2013) 064101.

**Prof. Chi Zhang** received his Ph.D. degree from Tsinghua University in 2009.After graduation, he worked in Tsinghua University as a postdoc research fellow and NSK Ltd., Japan as a visiting scholar. He now is the principal investigator of Tribotronics Group in Beijing Institute of Nanoenergy and Nanosystems, Chinese Academy of Sciences (CAS), Fellow of the NANOSMAT Society, Member of Youth Innovation Promotion Association, CAS, and Youth Working Committee Member of Chinese Society of Micro-Nano Technology. Prof. Chi Zhang's research interests are triboelectric nanogenerator, tribotronics, self-powered MEMS/NEMS, and applications in sensor networks, human-computer interaction and new energy technology. He has been awarded by NSK Sino-Japan Friendship Excellent Paper Award of Mechanical Engineering and granted by National Natural Science Foundation of China, Beijing Natural Science Foundation, China Postdoctoral Science Foundation, and CAS. He has published over 50 papers and attained 13 patents.

**Prof. Zhong Lin Wang** received his Ph.D from Arizona State University in physics. He now is the Hightower Chair in Materials Science and Engineering, Regents' Professor, Engineering Distinguished Professor and Director, Center for Nanostructure Characterization, at Georgia Tech. Dr. Wang has made original and innovative contributions to the synthesis, discovery, characterization and understanding of fundamental physical properties of oxide nanobelts and nanowires, as well as applications of nanowires in energy sciences, electronics, optoelectronics and biological science. His discovery and breakthroughs in developing nanogenerators established the principle and technological road map for harvesting mechanical energy from environment and biological systems for powering a personal electronics. His research on self-powered nanosystems has inspired the worldwide effort in academia and industry for studying energy for micro-nano-systems, which is now a distinct disciplinary in energy research and future sensor networks. He coined and pioneered the field of piezotronics and piezo-phototronics by introducing piezoelectric potential gated charge transport process in fabricating new electronic and optoelectronic devices. Details can be found at: www.nanoscience.gatech.edu.

Please cite this article in press as: C. Zhang, Z.L. Wang, Tribotronics—A new field by coupling triboelectricity and semiconductor, Nano Today (2016), http://dx.doi.org/10.1016/j.nantod.2016.07.004